Structure-activity relationships of actively FhuE transported rifabutin derivatives with potent activity against Acinetobacter baumannii

M. Maingot, M. Bourotte, A.C. Vetter, B. Schellhorn, K. Antraygues, H. Scherer, M. Gitzinger, C. Kemmer, G.E. Dale, O. Defert, et al.

Structure-activity relationships of actively FhuE transported rifabutin derivatives with potent activity against *Acinetobacter baumannii*

M. Maingot[1]*, M. Bourotte[2]*, A. C. Vetter[3*], B. Schellhorn[4], K. Antraygues[1], H. Scherer[1], M. Gitzinger[4], C. Kemmer[4], G.E. Dale[4], O. Defert[2], S. Lociuro[4], M. Brönstrup[3], N. Willand[1*,#] and V. Trebosc[4*,#]

[1] Univ. Lille, Inserm, Institut Pasteur de Lille, U1177 - Drugs and Molecules for Living Systems, 59000 Lille, France
[2] BioVersys SAS, 1 rue du Professeur Calmette, 59000 Lille, France
[3] Department of Chemical Biology, Helmholtz Centre for Infection Research, Inhoffenstraße 7, 38124 Braunschweig, Germany
[4] BioVersys AG, 60C Hochbergerstrasse, 4057 Basel, Switzerland

* equal contribution
# nicolas.willand@univ-lille.fr
# vincent.trebosc@bioversys.com

ABSTRACT

Hospital-acquired infections are on the rise and represent both, a clinical and financial burden. With resistance emerging and an ever-dwindling armamentarium at hand, infections caused by *Acinetobacter baumannii* are particularly problematic, since these bacteria have a high level of resistance and resilience to traditional and even last-resort antibiotics. The antibiotic rifabutin was recently found to show potent *in vitro* and *in vivo* activity against extensively drug resistant *A. baumannii.* Building on this discovery, we report on the synthesis and activity of rifabutin analogs, with a focus on *N*-functionalization of the piperidine ring. The antimicrobial testing uncovered structure activity relationships (SAR) for *A. baumannii* that were not reflected in *Staphylococcus aureus.* The cellular activity did not correlate with cell-free transcription inhibition, but with bacterial intracellular compound accumulation. Mass spectrometry-based accumulation studies confirmed the involvement of the siderophore receptor FhuE in active compound translocation at low concentrations, and they showed a strong impact of the culture medium on the accumulation of rifabutin. Overall, the study underlines the structural feature required for strong accumulation of rifabutin in *A. baumannii* and identifies analogs as or more potent than rifabutin against *A. baumannii*.

HIGHLIGHTS

- 35 spiropiperidyl rifabutin analogues were synthesized and tested
- Structural features for active internalization by *A. baumannii* were identified
- The role of FhuE in the transport of rifabutine analogues was confirmed

KEYWORDS

Ansamycin antibiotics; rifabutin; carbapenem-resistant *A. baumannii*; minimum inhibitory concentration; structure-activity relationships; compound uptake

GRAPHICAL ABSTRACT

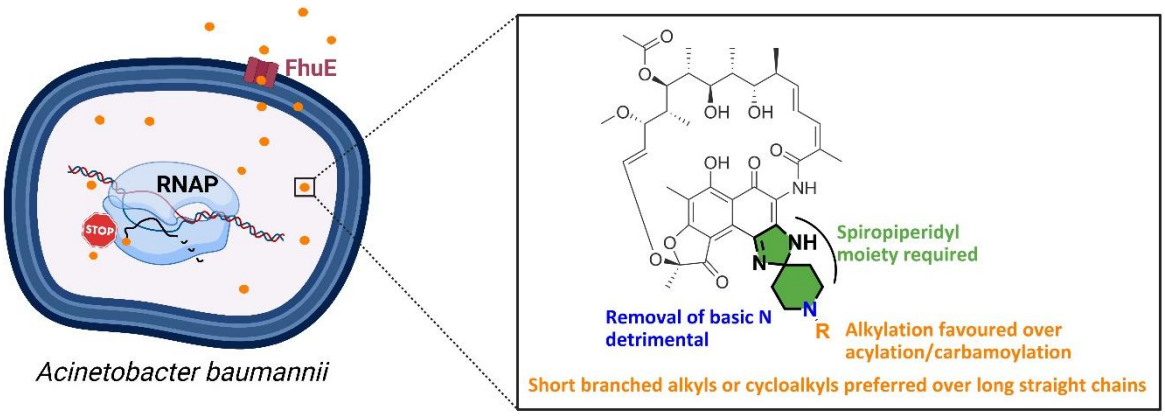

ABBREVIATIONS

Rbt = rifabutin, RNAP = RNA polymerase, RPMI = Roswell Park Memorial Institute, FCS = fetal calf serum

1. INTRODUCTION

The global spread of antibiotic resistant *Acinetobacter baumannii* strains has drastically limited the available options to treat infections caused by this Gram-negative pathogen.[1–3] Blood or lung infections caused by extensively drug-resistant *A. baumannii* have a mortality rate that can be above 50%,[4–6] which highlights that the antimicrobial arsenal is inadequate for such infections.[7] Accordingly, carbapenem-resistant *A. baumannii* has recently been included in the WHO priority list of pathogens against which novel therapeutic strategy are urgently needed.[8] In this context, screening of the ReFrame drug repurposing library identified the potent antibacterial activity of rifabutin (Rbt) toward *A. baumannii*.[9] Rbt was approved by the FDA in 1992 as an oral formulation for the prevention of disseminated *Mycobacterium avium* complex disease in patients with advanced HIV infection. A Rbt intravenous formulation (BV100) has been studied and is currently in clinical development for the treatment of severe infections caused by carbapenem-resistant *A. baumannii.*[10] In parallel more soluble prodrugs have also been designed and validated in mice to propose an alternative strategy for IV administration.[11]

Rbt is a semisynthetic compound derived from rifamycin SV (Figure 1). Rbt, similarly to other rifamycin derivatives, inhibits the initiation of bacterial transcription by binding to the β-subunit (RpoB) of the RNA polymerase (RNAP).[12] Despite the RNAP rifamycin-binding region being highly conserved in prokaryotes, the anti-bacterial spectrum of rifamycin antibiotics is primarily limited to mycobacteria and Gram-positive, because of the reduced capacity of these antibiotics to cross the outer membrane of most Gram-negative species.[13] However, Rbt was recently shown to exert an unexpected and potent activity against *A. baumannii* when tested in iron limited conditions, which was attributed to an active uptake mechanism across the outer membrane mediated by the TonB dependent siderophore receptor FhuE.[10,14] Importantly, the potent Rbt activity in iron-limited medium well-predicted Rbt efficacy *in vivo*.[15] This novel mode of action is specific for *A. baumannii*

and Rbt; none of the other Gram-negative species tested showed Rbt hyperactivity[16] and none of the several rifamycin drugs tested showed hyperactivity against *A. baumannii*.[9,14]

Structurally, rifamycins are ansamacrolides based on a rigid naphthoquinone/hydronaphtoquinone core bridged by an aliphatic ansa-chain (Figure 1). Hydroxyl groups at positions C-1, C-8, C-21 and C-23 cannot be modified without significantly affecting the antibacterial activity, because they form critical hydrogen bonds with the RNA polymerase.[17] Conversely, modelling and crystal structures of the rifamycin/RNAP complex showed that the 3,4-substituents of the naphthalene core extend toward an open space in the polymerase active site. Thus, modifications of the C-3 and C-4 positions are well tolerated and represent the best entry points to generate structurally diverse rifamycin derivatives.[17,18]

In this study, we report the synthesis of Rbt analogs focusing on the modification in the C-3/4 position together with their activities against several *A. baumannii* wildtype and mutant strains, and the bacterial uptake mechanisms that drive the observed structure-activity relationships (SAR). All analogs synthesized were tested in Roswell Park Memorial Institute (RPMI) 1640 medium supplemented with 10% fetal calf serum (FCS), since this iron-limited *in vitro* condition was previously described to allow overexpression of FhuE and internalization of only Rbt among all rifamycins.[14]

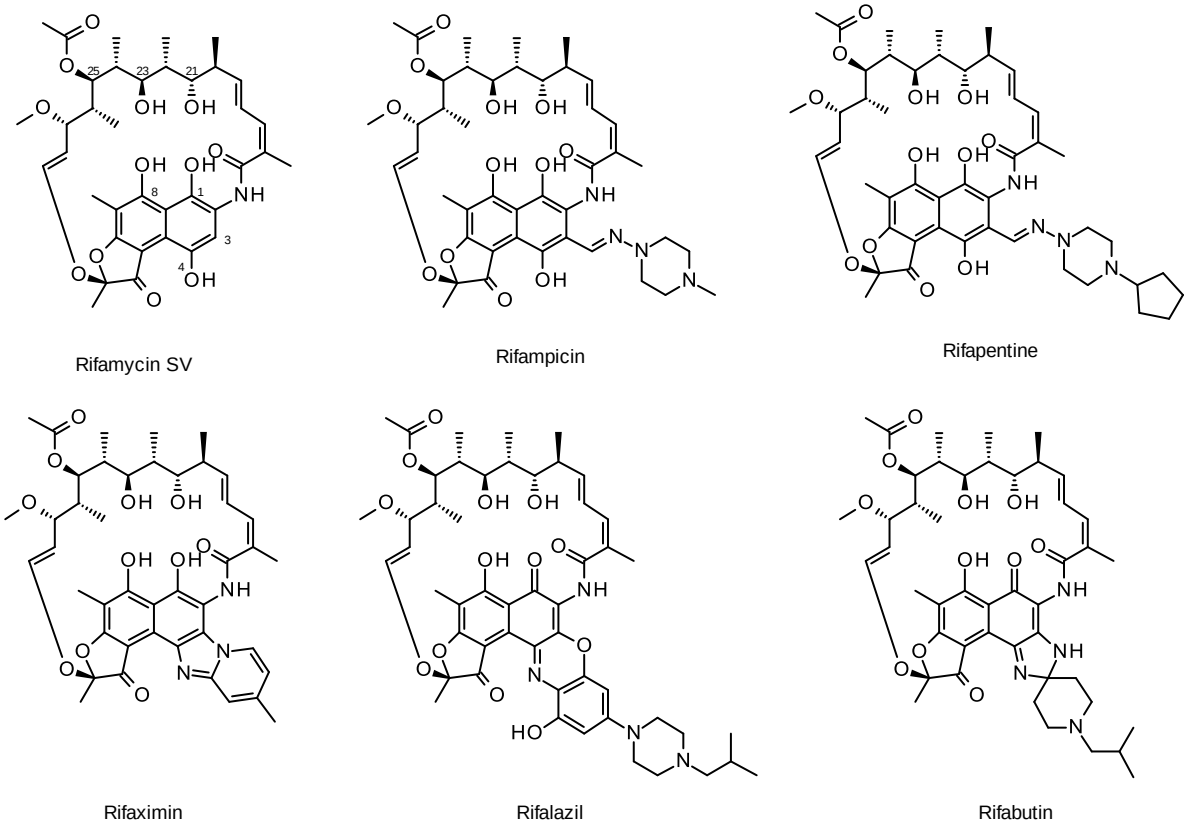

Figure 1: Chemical structures of rifamycin SV and analogues modified at the C3 and/or C4 position of the naphthalene core structure.

2. RESULTS and DISCUSSIONS

2.1. Structure-activity relationships study with C3/4 spirocyclic rifamycin derivatives against *A. baumannii*.

In order to rapidly establish initial SAR around modulations made at the C3/4 position of Rbt, condensations were undertaken between 3-amino-4-imino-rifamycin S and ketones using the two protocols described in **Scheme 1**. Compounds **2** to **6** and **27** to **41** were obtained using zinc and ammonium acetate in a solution of acetic acid and THF at room temperature (protocol **A**) with yields ranging from 23% to 78%. The synthesis of analogs **7** to **26** was performed in parallel on a 14 µmol scale using known synthetic protocol **B**.[19] Since neither the 3-amino-4-imino-rifamycin S (Table 1; MIC = 0.5 mg/L) nor the ketones had any low micromolar activity against *A. baumannii*, and overall purities of crude reactions estimated by HPLC analysis were greater than 70% (Table 1), the compounds were tested without any purification. Moreover, the most active analogs of this series were resynthesized and purified to confirm activities.

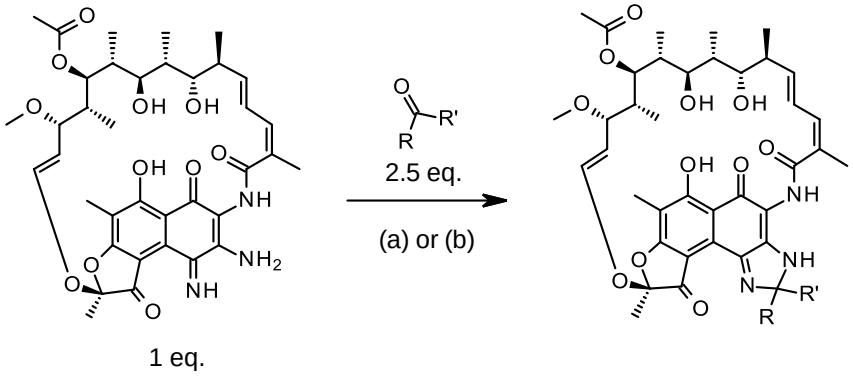

Scheme 1: **Synthesis of the 41 spirocyclic rifabutin analogs by condensation reaction between 3-amino-4-imino-rifamycin S and ketones.** Reagents and conditions; solution phase synthesis in round-bottomed flask: (a) Zn (2.5 eq.), $AcONH_4$ (2.5 eq.), AcOH (20 eq.), THF, rt; solution phase synthesis in Matrix™ plastic tube 1 mL: (b) Zn (2.5 eq.), $AcONH_4$ (2.5 eq.), THF, 40°C.

In a first round of SAR study, we compared the activity of Rbt with the non-alkylated spiropiperidyl analog compound **1** (Table 1): removal of the iso-butyl chain led to a drastic 250-fold decrease in potency, shifting from a MIC of 0.001 mg/L to a MIC of 0.25 mg/L. Replacement of the nitrogen of the piperidine by a methylene (compound **2**) led to 2-fold increase in potency, whereas introduction of an oxygen (compound **3**) led to a 10-fold decrease in potency. Moreover, dimethylation of the nitrogen atom of the piperidine (compound **4**), acylation (compound **5**) or carbamoylation (compound **6**) all led to less potent analogs. Together, these data show that only the introduction of a piperidine or a cyclohexyl at the C3/4 position of 3-amino-4-imino-rifamycin S helps to maintain a MIC lower than 1 mg/L. We therefore turned our attention on the synthesis of a focused library of *N*-alkylated analogues of Rbt using parallel solution phase synthesis (compounds **7**-**26**; Table 1).

Table 1: Activity of the spirocyclic rifabutin analogs on *A. baumannii* HUMC1.

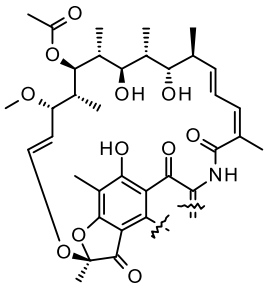

Cpd	substituent	Purity (%)	Yield (%)	MIC[c] (mg/L)	Cpd	substituent	Purity (%)	Yield (%)	MIC[d] (mg/L)
Rbt	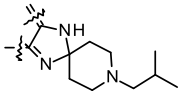	-	-	0.001	**22**[b]	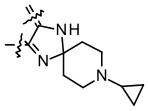	77	-	≤ 0.002
3-amino-4-imino-rifamycin S	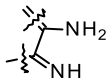	-	-	0.5	**22**[c]	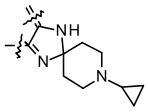	99	57	0.001
1[a]	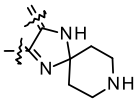			0.25	**23**[b]	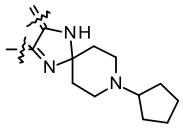	83	-	≤ 0.002
2[a]	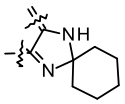	97	25	0.125	**23**[c]	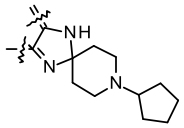	99	59	0.004
3[a]	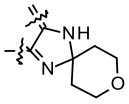	97	26	2	**24**[b]	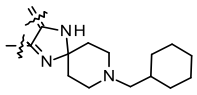	73	-	0.06
4[a]	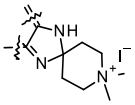	97	26	8	**24**[c]	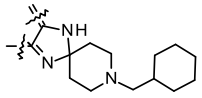	99	75	0.03
5[a]	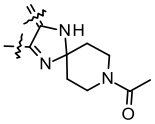	97	38	4	**25**[b]	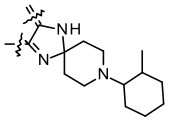	100	-	0.125
6[a]	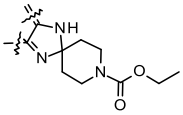	97	45	8	**26**[b]	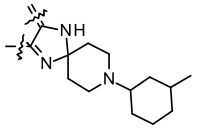	76	-	0.03
7[b]	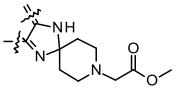	88	-	0.5	**27**[a]	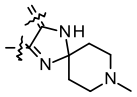	99	42	0.016
8[b]	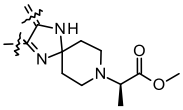	93	-	0.125	**28**[a]	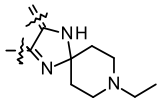	96	23	0.004

9[b]	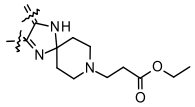	81	-	1	**29**[a]	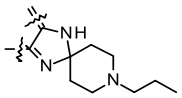	99	49	0.004
10[b]	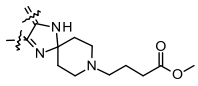	77	-	0.5	**30**[a]	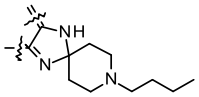	99	49	0.004
11[b]	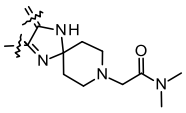	82	-	0.5	**31**[a]	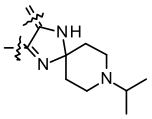	99	61	0.002
12[b]	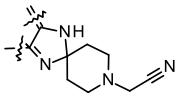	59	-	0.25	**32**[a]	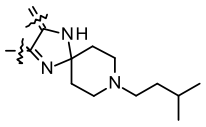	99	67	0.016
13[b]	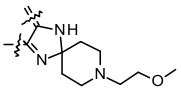	70	-	0.016	**33**[a]	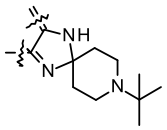	99	48	0.002
14[b]	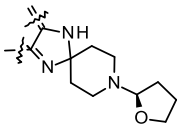	82	-	0.016	**34**[a]	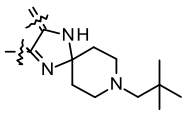	98	61	0.008
15[b]	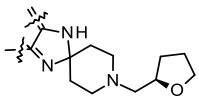	82	-	0.125	**35**[a]	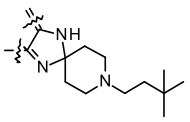	99	72	0.06
16[b]	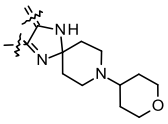	82	-	0.008	**36**[a]	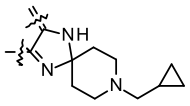	99	67	0.001
17[b]	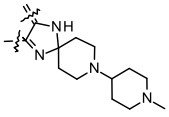	76	-	0.25	**37**[a]	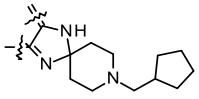	99	60	0.016
18[b]	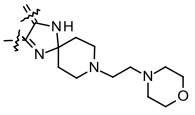	78	-	1	**38**[a]	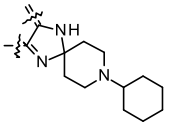	99	65	0.016
19[b]	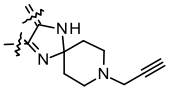	82	-	0.008	**39**[a]	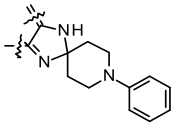	97	38	0.125
20[b]	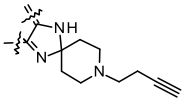	70	-	0.004	**40**[a]	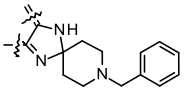	99	68	0.125

21[b]	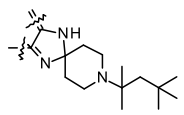	78	-	0.03	**41**[a]	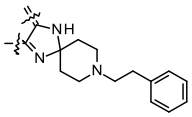	99	78	0.5

[a] Compounds were synthesized using protocol A; [b] compounds were synthesized in parallel using protocol B; [c] Compounds were re-synthesized using protocol A; [d] MIC were obtained in RPMI + 10% FCS.

Introduction of esters at various distances from the nitrogen atom (compounds **7-10**), amide (compound **11**), nitrile (compound **12**) or piperidine (compound **17**) did not improve the potency compared with the non-substituted piperidine analog (compound **1**). However, introduction of non-basic heterocycles such as morpholine (compound **16**) or tetrahydrofuran (compound **14**) led to compounds with MICs of 0.008 and 0.016 mg/L, respectively. Addition of methylene spacers (compounds **18** and **15**) was detrimental to the activity. Finally, cyclisation was not essential since the introduction of a methoxymethyl group (compound **13**, MIC = 0.016 mg/L) was sufficient to maintain a potency in the low micromolar range.

Hydrophobic substituents were generally well tolerated with the propyne (compound **19**), butyne (compound **20**), cyclopropyl (compound **22**) and cyclopentyl (compound **23**) derivatives displaying activity in the same range as Rbt (1- to 8-fold shift). Interestingly, introduction of steric hindrance (compound **21**) or large alicyclic moieties (compounds **24**, **25** and **26**) led to less potent analogs. From this second series of Rbt derivatives, cyclopropyl (compound **22**) and cyclopentyl (compound **23**) analogs were found equipotent to Rbt. These two compounds were resynthesized, purified and characterized by NMR. Compound **22** was as potent as Rbt while compound **23** was 4-times less potent.

To further evaluate the impact of hydrophobic substituents, aliphatic and aromatic analogs were considered with a focus on the length of aliphatic chains, their branching and the size of the aliphatic rings introduced (compounds **27-41**, Table 1). As previously observed, alkyl substitution of the piperidine nitrogen is required to improve potency. Indeed, the methyl analog (compound **27**) was 16-fold more potent than the non-substituted piperidine analog (compound **1**). Carbon chain elongation enhanced activity even further, with the ethyl analog (compound **28**) having a MIC of 0.004 mg/L. However, the addition of one (propyl analog, compound **29**) and two extra carbons (butyl analog, compound **30**) did not afford more potent compounds. Introduction of methyl substituents at the α-position of the nitrogen enhanced activity. The iso-propyl (compound **31**) and tert-butyl (compound **33**) analogs showed MIC of 0.002 mg/L. Conversely, the elongation of the carbon chains led to a decrease in potency. A 16-fold MIC increase was observed shifting from iso-butyl (Rbt) to iso-pentyl (compound **32**), a 4-fold MIC increase shifting from tert-butyl (compound **33**) to tert-pentyl (compound **34**), and an 8-fold MIC increase shifting from tert-pentyl (compound **34**) to tert-hexyl (compound **35**).

The cyclopropyl analogs, either directly connected (compound **22**) or linked through a methylene (compound **36**) to the piperidine ring were as potent as Rbt, while their analogs in the cyclopentyl series (compounds **23** and **37**, respectively) and cyclohexyl series (compounds **38** and **24**, respectively) were all less potent. Finally, the introduction of aromaticity (compounds **39** - **41**) led to a 125- to 500-fold decreased potency compared with Rbt. Altogether, these results indicate that steric hindrance near the nitrogen atom of the piperidine is beneficial for potency against

A. baumannii, while introduction of large aliphatic or aromatic 5- and 6-membered rings lead to higher MICs.

2.2. FhuE is required for potent activity of the Rbt analogs.

Rifamycin antibiotics, including Rbt, exert potent *in vitro* activity against the Gram-positive pathogen *S. aureus*.[20] Therefore, we determined the MIC of the Rbt analogs against *S. aureus* to evaluate whether the SAR observed with *A. baumannii* is conserved. All the compound tested in this series show either an equal (compounds **24**, **29**, **30**, **32**, **33**, **36**, **40**, **41**), 2- to 4-fold lower (compounds **22**, **23**, **28**, **31**, **34**, and **27**, **35**) or 2- to 4-fold higher (compounds **37**, **38**, **39** and **1**) MIC than Rbt (MIC = 0.016 mg/L), indicating that changes in chain length, branching and the nature of the rings introduced have a minor impact on activity against *S. aureus* as opposed to *A. baumannii* (Figure 2A).
These results confirm that modifications of Rbt at C-3/4 positions are generally tolerated for activity against *S. aureus*, which is in agreement with the similar activity range observed for the commercially available rifamycin drugs against this species.[20] It is widely assumed that rifamycins reach the cytoplasm of *S. aureus* by passive diffusion through the cytoplasmic membrane,[21] as opposed to *A. baumannii* where Rbt is actively transported through the outer membrane via FhuE,[14] suggesting that the *A. baumannii* specific SAR observed with the Rbt analogs is FhuE dependent.
Additionally, Rbt analogs were tested on *A. baumannii* strains encoding mechanisms that lead to elevated Rbt MIC, such as RpoB mutations or *fhuE* deletion.[14] The majority of the Rbt analogs tested retained potent activity on the two RpoB mutants with MICs ranging from 0.004 mg/L (compound **22**) to 1 and 2 mg/L (compound **1** and **35**) and the SAR observed on the wild-type strain were conserved (Figure 3). Conversely, the *A. baumannii* mutant where *fhuE* was deleted was less sensitive to the whole series of analogs with MICs ranging from 0.5 mg/L to 4 mg/L and the SAR observed on the wild-type strain were not conserved, confirming that the SAR is driven by a FhuE-mediated active transport in *A. baumannii* (Figure 2B).
Interestingly, the cyclopropyl analog (compound **22**) showed the best activity on the RpoB mutants, with a MIC 2- to 8-fold lower than that of Rbt. Amino acid mutations in RpoB interfere with the binding of rifamycins to the RNAP, suggesting that compound **22** may conserve its binding to the RpoB mutants, as previously described for other rifamycin analogs.[22,23] Alternatively, a better cellular uptake of the analog compared to Rbt, allowing increased intracellular concentration near the target potentially compensating the lower affinity for the mutated RNAP, might be another reason for this enhanced activity.

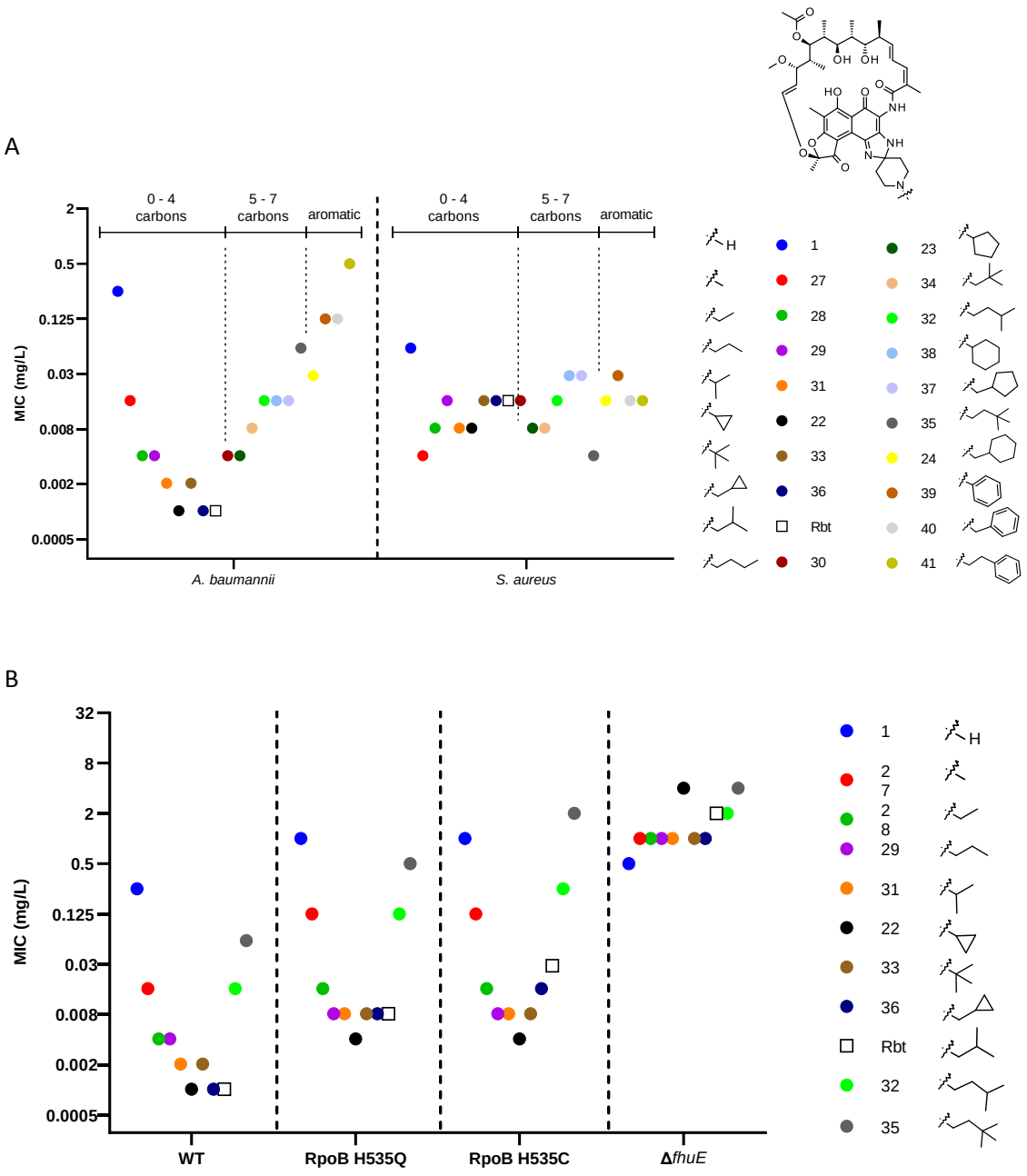

Figure 2: Structure-activity relationships of selected rifabutin analogs on *A. baumannii* and *S. aureus* strains. A) The MIC of the analogs was determined using microbroth dilution in RPMI supplemented with 10% FCS for *A. baumannii* HUMC1 and in CAMHB for *S. aureus* UAMS-1625. The analogs were sorted by the number of carbon atoms that are present in the linear, branched or cyclic alkyl chains attached on the nitrogen of the piperidine scaffold. B) The MIC of the analogs was determined using microbroth dilution in RPMI supplemented with 10% FCS on *A. baumannii* HUMC1 wildtype strain (WT) and on *A. baumannii* strains encoding the RpoB H535Q mutation, the RpoB H535C mutation and a *fhuE* deletion (Δ*fhuE*).

2.3. Inhibition of transcription is not the SAR driver for Rbt analogs.

To confirm that the cell-based SAR observed in this chemical series against *A. baumannii* are only FhuE dependent, two potent analogs (compounds **22** and **33**) and two less active analogs (compounds **1** and **35**) were tested in a cell-free transcription assay. Their cell-free transcription inhibition activities were within a 4-fold range (0.05 to 0.17 mg/L) and similar to the transcription inhibition activity of Rbt and rifampicin (0.07 mg/L) (Table 2). In contrast, there was a 250-fold shift in MIC between the most and the least potent of the tested analogs, indicating that there is no correlation between cell-based activity and transcription inhibition activity. The same conclusion can be drawn by comparing the activities of Rbt and rifampicin. The absence of correlation between cell-based and cell-free activity is indirectly suggesting that the SAR observed with the Rbt analogs is due to a differential FhuE-mediated uptake in *A. baumannii*.

Table 2: Cell-based (MIC) and cell-free activity of selected rifabutin analogs on *A. baumannii* HUMC1.

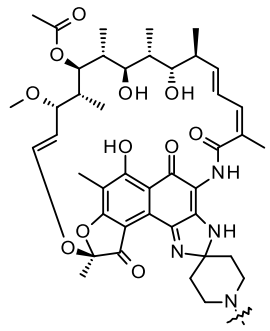

Compound	substituent	MIC in RPMI+FCS (mg/L)	Cell-free IC_{50} (mg/L)[a]
Rbt		0.001	0.07
1		0.25	0.05
22		0.001	0.12
33		0.002	0.06
35	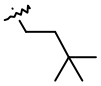	0.06	0.17
Rifampicin		4	0.07

[a] average of at least three biological replicates.

2.4. Intracellular accumulation of Rbt and its analogs correlates with *in vitro* activity.

The lack of a detailed understanding of compound accumulation poses a key obstacle in the development of drugs against Gram-negative bacteria.[24,25] In light of this, we conducted a comprehensive study of whole cell (WC) accumulation of Rbt in *A. baumannii.* First, to assess how culture medium affects the amount of Rbt internalized, WC accumulation of different concentrations of Rbt in *A. baumannii* HUMC1 and *A. baumannii* HUMC1 Δ*fhuE* was studied using an LC-MS/MS based approach. At the lowest concentrations studied (0.002 µM to 0.02 µM), bacterial uptake, expressed in ng of Rbt per 5 mL bacterial suspension, was observed when *A. baumannii* HUMC1 was cultured in iron-limited RPMI medium supplemented with 10% FCS (Figure 3A). In contrast, accumulation was observed only at concentrations ≥ 0.05 µM when the strain was grown in iron rich cation-adjusted Mueller Hinton broth (CAMHB). Regardless of the culture medium, Rbt accumulation in *A. baumannii* HUMC1 Δ*fhuE* fell below the limit of detection at low Rbt concentrations (< 0.02 µM) and uptake increased with increasing Rbt concentration (Figure 3B). Thus, the culture medium was found to have a strong effect on the accumulation of Rbt in the wildtype strain but not in the Δ*fhuE*

strain. Moreover, at low concentrations and under iron-depleted conditions, the *fhuE*-deleted strain internalized significantly less Rbt than the wild type strain. These findings are in line with previous studies, that reported a strong dependency of antibiotic activity on the culture medium and on FhuE.[9,14]

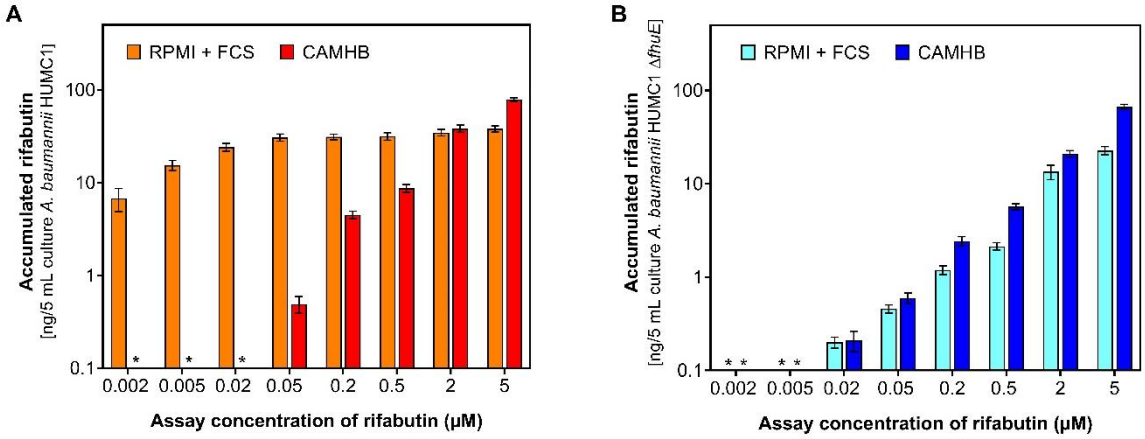

Figure 3: Whole cell accumulation of rifabutin in rich and iron-limited conditions. Whole cell accumulation of rifabutin in *A. baumannii* HUMC1 (A) and *A. baumannii* HUMC1 Δ*fhuE* (B) cultured in RPMI + 10% FCS and CAMHB; bars are representative of the average amount in ng of Rbt internalized by 5 mL bacterial suspension at OD_{600} = 0.8. Cells were incubated at the indicated concentration for 10 minutes at 37 °C (n ≥ 2 independent replicates in duplicate/triplicate, error bars = ± SEM); ***** = no quantifiable amount of compound detected.

Next, to confirm that Rbt was internalized by the bacterial cells, *A. baumannii* HUMC1 cultured under iron-limited conditions was incubated with 0.005 µM Rbt and subjected to subcellular fractionation. As illustrated in Figure 4A, most Rbt was detected in the cytoplasmic fraction (79% of the sum of fractions) where the drug's target is located, while 20% was detected in the membrane fraction (comprising both inner and outer membranes) and < 1% was found in the periplasm.

Finally, we studied the accumulation of selected Rbt analogs in *A. baumannii* HUMC1. Like in the cell-free transcription inhibition assays, two potent (compounds **22** and **33**) and two less active analogs (compounds **1** and **35**) were used in the WC accumulation assay alongside benchmark compounds Rbt and rifampicin (Figure 4B). Using conditions enabling active FhuE-mediated transport, cells were cultured under iron-limited conditions and incubated with the compounds at 0.05 µM (saturated uptake, see Figure 3A). Overall, uptake, expressed as pmol/5 mL bacterial suspension, was highest for Rbt, its structural isomer compound **33** and compound **22** (Figure 4B). Compared to Rbt and compound **33**, accumulation of compound **35** was approximately threefold lower, but 20-fold higher than the uptake of compound **1**, while the uptake of rifampicin fell below the limit of detection. Thus, in line with the SAR discussed earlier, the introduction of branching groups no further than one methylene group away from the piperidinic nitrogen favours uptake (Rbt, compounds **22** and **33**), while an additional methylene unit as in compound **35** and lack of the spiropiperidyl moiety (rifampicin) are detrimental. In all cases, the biological activity, expressed here as inverse MIC (Figure 4B, patterned bars), correlated well with compound uptake.

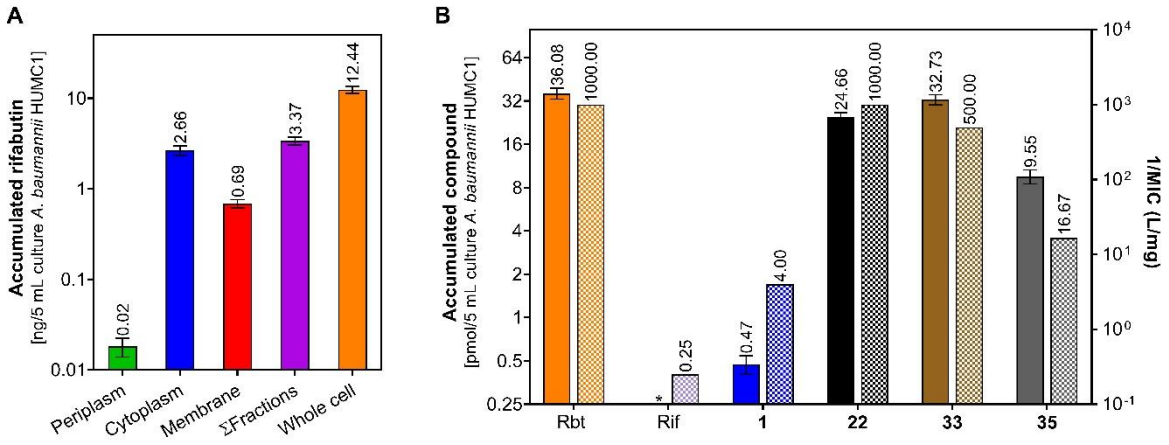

Figure 4: Accumulation of rifabutin and analogs in *A. baumannii* HUMC1. A) Accumulation of rifabutin in subcellular compartments. Cells were cultured in RPMI + 10% FCS and incubated with rifabutin (0.005 µM) for 10 minutes at 37 °C (n = 4 independent replicates in duplicate), bars are representative of the average amount in ng of Rbt internalized by 5 mL bacterial suspension at OD_{600} = 0.8; B) Whole cell uptake of rifabutin derivatives in *A. baumannii* HUMC1: cells were cultured in RPMI + 10% FCS and incubated with compound (0.05 µM) for 10 minutes at 37 °C (n ≥ 2 independent replicates in duplicate), patterned bars = 1/MIC, * no quantifiable amount of compound detected, Rbt: rifabutin, Rif: rifampicin, bars are representative of the average picomoles of compound internalized by 5 mL bacterial suspension at OD_{600} = 0.8; error bars = ± SEM.

3. CONCLUSION

The development of novel antibiotics is often encumbered by challenges on achieving intracellular translocation, in particular for Gram-negative bacteria featuring an inner and outer cell membrane.[25–27] With the recent finding that Rbt penetrates *A. baumannii* by hijacking the outer membrane siderophore receptor protein FhuE,[3,4] a new starting point for the development of potentially active compounds surfaced. In this context, 35 spiro-piperidyl substituted Rbt derivatives were prepared and evaluated to derive structure-activity relationships. These can be summarized as follows: (i) *N*-substitution is required for high activity, with non-polar substituents yielding more active analogs, (ii) the size of the substituent plays a critical role, with alkyl groups containing up to four carbons performing best, (iii) bulky groups outperform their straight chain isomers, although remote branching impairs activity.

The observed SAR were neither conserved in *A. baumannii* deleted for *fhuE* nor in *S. aureus,* inherently lacking FhuE due to the absence of outer membrane. In addition, there was no correlation between cell-based activity and transcription inhibition activity, altogether suggesting that the observed SAR is driven by FhuE-mediated uptake in *A. baumannii*. Intracellular accumulation data confirmed that the observed diminished activity of analogs is a direct result of the compounds failure to efficiently cross the cell envelope. Active FhuE-mediated transport leads to a massively enhanced accumulation at low Rbt concentrations (< 1 mg/L) compared to a FhuE-deficient strain, which is in line with the low Rbt MIC (< 0.125 mg/L) of strains with functional uptake when tested on large strain panel.[14]

In summary, the study demonstrates FhuE-dependent structure-activity relationships for Rbt analogues, with C3/4 modifications, that are specific for *A. baumannii*. It also underlines the

importance of taking compound accumulation information into account for an understanding of antibiotic activity.

4. Experimental section

4.1. Chemistry

Rifabutin was provided by BioVersys. Derivative 1 and 3-amino-4-imino-rifamycin S were purchased from AlfaChemistry. Reagents and solvents for synthesis, analysis or purification were purchased from commercial suppliers and used without further purification. Progress of all reactions was routinely monitored by thin layer chromatography (TLC) and/or by High Performance Liquid Chromatography - Mass Spectrometry (HPLC-MS). TLC was performed using Merck® commercial aluminum sheets coated with silica gel 60 F254. Visualization was achieved by fluorescence quenching under UV light at 254 nm or stained by potassium permanganate. Purifications were performed by flash chromatography, reverse chromatography or preparative HPLC. Flash chromatography purifications were done on prepacked columns Reveleris® flash cartridges (40 µm, Büchi® FlashPure or 15-40 µM, Macherey-Nagel® Chromabond) under pressure with an Interchim Puriflash® 430 instrument. Products were detected by UV absorption at 254 nm and by ELSD. HPLC-MS analysis was performed on LC-MS Waters Alliance Micromass ZQ 2000 system equipped with a Waters 2747 sample manager, a Waters 2695 separations module, a Waters 2996 photodiode array detector (210-400 nm at a 1.2 nm resolution) and a Waters Micromass ZQ2000 detector (scan 100-800). XBridge C18 column (3.5 µm particle size, dimensions 50 mm x 4.6 mm) was used for HPLC analysis. The injection volume was 20 µL. For a 5 min analysis, the elution was done at pH = 3.8 from 100% H_2O/0.1% ammonium formate to 2% H_2O/98% CH_3CN/0.1% ammonium formate over 3.5 min. A flow rate at 2 mL/min was used. For a 30 min analysis, the elution was done at pH = 3.8 from 100% H_2O/0.1% ammonium formate to 2% H_2O/98% CH_3CN/0.1% ammonium formate over 7 min. A flow rate at 1 mL/min was used. Purity (%) was determined by reversed phase HPLC, using UV detection (215 and 254 nm). HRMS analysis were performed on a LCT Premier XE Micromass, using a C18 X-Bridge 3.5 µm particle size column, dimensions 50 mm * 4.6 mm. A gradient starting from 98% H_2O 5 mM ammonium formate pH=3.8 and reaching 100% CH_3CN 5 mM ammonium formate pH = 3.8 within 3 min at a flow rate of 1 mL/min was used. NMR spectra were recorded on a Bruker® Avance-300 spectrometer. Chemical shifts were measured in ppm relative to the specific solvent signal [e.g. 7.26 (residual $CDCl_3$) and 77.16 ($CDCl_3$) ppm for ^1H and ^{13}C NMR spectra, respectively]. The assignments were made using one-dimensional (1D) ^1H and ^{13}C spectra and two-dimensional (2D) HSQC-DEPT, COSY and HMBC spectra. NMR coupling constants (*J*) are reported in Hertz (Hz), and splitting patterns are indicated as follows: s (singlet), brs (broad singlet), d (doublet), dd (doublet of doublets), ddd (doublet of doublets of doublets), dt (doublet of triplets), t (triplet), td (triplet of doublets), q (quartet), m (multiplet).

4.1.1. General procedure used for the synthesis of rifabutin analogs 2-6, 22-24 and 27-41

To a 0.3M solution of 3-amino-4-imino-rifamycin S (1 eq) in THF was added the corresponding ketone (2.5 eq), followed by ammonium acetate (2.5 eq), zinc (2.5 eq) and acetic acid (20 eq). Reaction was stirred at room temperature. After 30min, mixture was filtered and solvent was evaporated. DCM was added. Then, organic layer was washed with a saturated solution of $NaHCO_3$, brine, dried over $MgSO_4$ and concentrated under vacuum. The obtained solid was purified by chromatography ($CHCl_3$/NH_3 in MeOH - 2N) to give the expected product as a purple solid.

Compound 2 : the title compound was obtained as a purple solid (yield = 25%) following the general procedure and using cyclohexanone as ketone. LC/MS (ESI+): tr = 15.10 min, m/z $[M+H]^+$ = 790.21. UV purity: 97 % (254 nm). HRMS (Maldi-TOF): m/z calculated for $[M+H]^+$ = 790.3915; found for $[M+H]^+$ = 790.3911. ^{1}H NMR (300 MHz, $CDCl_3$): δ -0.07 (d, *J* = 7.0 Hz, 3H), 0.59 (d, *J* = 6.9 Hz, 3H), 0.82 (d, *J* = 6.9 Hz, 3H), 1.02 (d, *J* = 7.0 Hz, 3H), 1.39-1.47 (m, 1H), 1.57-1.75 (m, 8H), 1.73 (s, 3H), 1.89-2.09 (m, 4H), 1.99 (s, 3H), 2.04 (s, 3H), 2.28-2.42 (m, 1H), 2.31 (s, 3H), 2.95-3.03 (m, 1H), 3.06 (s, 3H), 3.32 (dd, *J* = 7.2, 2 .6 Hz, 1H), 3.44 (s, 1H), 3.63 (d, *J* = 5.8 Hz, 1H), 3.67 (d, *J* = 10.1 Hz, 1H), 4.76 (dd, J = 10.2, 1.2 Hz, 1H), 5.15 (dd, *J* = 12.5, 7.3 Hz, 1H), 6.01 (d, *J* = 15.6, 6.7 Hz, 1H), 6.15 (d, *J* = 12.5 Hz, 1H), 6.23 (d, *J* = 10.4 Hz, 1H), 6.36 (dd, *J* = 15.6, 10.4 Hz, 1H), 8.20 (s, 1H), 9.19 (brs, 1H), 14.79 (s, 1H). ^{13}C NMR (75 MHz, $CDCl_3$): δ 7.7, 8.8, 10.9, 11.3, 17.5, 20.3, 21.1, 21.9, 24.0, 25.0, 29.8, 33.1, 35.8, 36.7, 37.8, 38.2, 56.9, 72.8, 73.3, 77.0, 80.7, 96.4, 104.4, 107.3, 108.9, 111.9, 114.2, 116.1, 124.1, 125.3, 131.4, 133.1, 141.1, 142.4, 144.2, 154.9, 168.3, 168.6, 171.6, 172.2, 180.9, 192.7.

Compound 3 : the title compound was obtained as a purple solid (yield = 26%) following the general procedure and using tetrahydropyran-4-one as ketone. LC/MS (ESI+): tr = 12.85 min, m/z $[M+H]^+$ = 792.37. UV purity: 97 % (254 nm). HRMS (Maldi-TOF): m/z calculated for $[M+H]^+$ = 792.3707; found for $[M+H]^+$ = 792.3701. ^{1}H NMR (300 MHz, $CDCl_3$): δ -0.09 (d, *J* = 7.1 Hz, 3H), 0.57 (d, *J* = 7.2 Hz, 3H), 0.81 (d, *J* = 6.9 Hz, 3H), 1.01 (d, *J* = 7.0 Hz, 3H), 1.37-1.49 (m, 1H), 1.54-1.63 (m, 1H), 1.67-1.86 (m, 3H), 1.73 (s, 3H), 1.99 (s, 3H), 2.02 (s, 3H), 2.06-2.19 (m, 2H), 2.28-2.41 (m, 1H), 2.32 (s, 3H), 2.94-3.02 (m, 1H), 3.05 (s, 3H), 3.32 (dd, J = 7.1, 2.0 Hz, 1H), 3.53 (s, 1H), 3.61-3.71 (m, 2H), 3.92-4.02 (m, 2H), 4.16-4.32 (m, 2H), 4.75 (dd, *J* = 10.7, 1.4 Hz, 1H), 5.09 (dd, *J* = 12.5, 7.1 Hz, 1H), 5.98 (dd, *J* = 15.6, 6.7 Hz, 1H), 6.14 (dd, *J* = 12.5, 0.8 Hz, 1H), 6.24 (dd, *J* = 10.4, 1.3 Hz, 1H), 6.35 (dd, *J* = 15.6, 10.4 Hz, 1H), 8.33 (s, 1H), 8.86 (s, 1H), 14.62 (s, 1H). ^{13}C NMR (75 MHz, $CDCl_3$): δ 7.7, 8.8, 10.8, 11.2, 17.4, 20.4, 21.0, 21.8, 33.0, 36.3, 37.0, 37.6, 37.7, 38.2, 57.0, 65.6, 65.7, 72.6, 73.2, 76.9, 80.5, 93.2104.8, 107.3, 108.9, 111.7, 114.5, 115.6, 124.1, 125.1, 131.0, 133.3, 141.0, 142.0, 144.1, 155.6, 168.2, 168.5, 171.6, 172.3, 181.6, 192.7.

Compound 4 : the title compound was obtained as a purple solid (yield = 26%) following the general procedure and using 1,1-Dimethyl-4-oxopiperidin-1-ium iodide as ketone. LC/MS (ESI+): tr = 10.65 min, m/z $[M]^+$ = 819.48. UV purity: 97 % (254 nm). HRMS (Maldi-TOF): m/z calculated for $[M]^+$ = 819.4175; found for $[M]^+$ = 819.4169.

Compound 5: the title compound was obtained as a purple solid (yield = 38%) following the general procedure and using 1-acetylpiperidin-4-one as ketone. LC/MS (ESI+): tr = 11.98 min, m/z $[M+H]^+$ = 833.51. UV purity: 97 % (254 nm). HRMS (Maldi-TOF): m/z calculated for $[M+H]^+$ = 833.3973; found for $[M+H]^+$ = 833.3956. ^{1}H NMR (300 MHz, $CDCl_3$): δ -0.07 (d, *J* = 7.1 Hz, 3H), 0.06 (d, *J* = 6.1 Hz, 3H), 0.58 (d, *J* = 6.8 Hz, 3H), 0.59 (d, *J* = 6.8 Hz, 3H), 0.81 (d, *J* = 6.9 Hz, 1H), 0.82 (d, J = 6.9 Hz, 1H), 1.01 (d, *J* = 7.0Hz, 1H), 1.02 (d, *J* = 7.0Hz, 1H), 1.36-1.59 (m, 2H), 1.67-1.84 (m, 12H), 1.99 (s, 6H), 2.01 (s, 6H), 2.04-2.13 (m, 4H), 2.16 (s, 6H), 2.28-2.41 (m, 2H), 2.31 (s, 6H), 2.93-3.03 (m, 2H), 3.08 (s, 6H), 3.27-3.36 (m, 2H), 3.47-3.72 (m, 8H), 3.80-4.09 (m, 4H), 4.40-4.55 (m, 2H), 4.68-4.79 (m, 2H), 5.07 (dd, *J* = 7.2, 1.8 Hz, 1H), 5.11 (dd, *J* = 7.3, 1.8 Hz, 1H), 5.94 (dd, *J* = 6.7, 2.9 Hz, 1H), 5.99 (dd, *J* = 6.6, 3.1 Hz, 1H), 6.14 (d, *J* = 12.5 Hz, 2H), 6.24 (dd, *J* = 10.3, 1.3 Hz, 2H), 6.28-6.41 (m, 2H), 8.32 (s, 2H), 8.73 (s, 1H), 8.78 (s, 1H), 14.53 (s, 1H), 14.55 (s, 1H). ^{13}C NMR (75 MHz, $CDCl_3$): δ 7.7, 8.8, 10.8, 11.0, 11.2, 11.3, 17.4, 20.3, 20.4, 21.0, 21.5, 21.9, 22.0, 33.0, 35.5, 36.3, 36.4, 37.2, 37.6, 37.7, 38.3, 39.6, 39.7, 44.5, 56.9, 72.6, 72.7, 73.1, 73.2, 76.9, 77.0, 80.7, 93.7, 93.8, 105.1, 105.2, 107.4, 107.5, 109.0, 111.7, 114.7, 115.4, 115.5, 124.1, 124.9, 125.0, 130.9, 131.0, 133.4, 133.5, 141.0, 141 .2, 141.8, 141.9,

144.3, 144.4, 155.8, 156.0, 168.20, 168.22, 168.57, 168.59, 169.0, 169.2, 171.5, 171.6, 172.3, 172.5, 181.7, 181.8, 192.7, 192.8.

Compound 6 : the title compound was obtained as a purple solid (yield = 45%) following the general procedure and using ethyl 4-oxopiperidine-1-carboxylate as ketone. LC/MS (ESI+): tr = 13.97 min, m/z $[M+H]^+$ = 863.36. UV purity: 97 % (254 nm). HRMS (Maldi-TOF): m/z calculated for $[M+H]^+$ =863.4079 ; found for $[M+H]^+$ = 863.4108. ^{1}H NMR (300 MHz, $CDCl_3$): δ -0.08 (d, *J* = 7.1 Hz, 3H), 0.58 (d, *J* = 6.8 Hz, 3H), 0.80 (d, *J* = 6.9 Hz, 3H), 1.00 (d, *J* = 7.0 Hz, 3H), 1.27 (t, J = 7.0 Hz, 1H), 1.32-1.45 (m, 1H), 1.46-1.57 (m, 1H), 1.68-1.82 (m, 3H), 1.71 (s, 3H), 1.95-2.08 (m, 2H), 1.98 (s, 3H), 2.01 (s, 3H), 2.30 (s, 3H), 2.32-2.39 (m, 1H), 2.93-3.01 (m, 1H), 3.05 (s, 3H), 3.31 (dd, *J* = 7.0, 2.1 Hz, 1H), 3.50 (s, 1H), 3.59-3.67 (m, 2H), 2.68-3.81 (m, 2H), 3.94-4.11 (m, 2H), 4.16 (dd, *J* = 14.2, 7.0 Hz, 1H), 4.73 (d, *J* = 10.5 Hz, 1H), 5.09 (dd, *J* = 12.5, 7.3 Hz, 1H), 5.96 (dd, *J* = 15.4, 6.7 Hz, 1H), 6.13 (dd, *J* = 12.5, 0.7 Hz, 1H), 6.23 (dd, *J* = 10.3, 1.2 Hz, 1H), 6.34 (dd, *J* = 15.4, 10.3 Hz, 1H), 8.31 (s, 1H), 8.80 (brs, 1H), 14.57 (s, 1H). ^{13}C NMR (75 MHz, $CDCl_3$): δ 7.7, 8.8, 10.9, 11.2, 14.8, 20.3, 21.0, 21.9, 33.0, 35.6, 36.4, 37.6, 38.3, 41.9, 56.9, 61.7, 72.6, 73.2, 76.9, 80.7, 93.9, 105.0, 107.4, 108.9, 111.7, 114.6, 115.5, 124.1, 125.0, 131.0, 133.3, 141.0, 141.9, 144.3, 155.6, 155.7, 168.1, 168.5, 171.5, 172.3, 181.6, 192.6.

Compound 22 : the title compound was obtained as a purple solid (yield = 57%) following the general procedure and using 1-cyclopropylpiperidin-4-one as ketone. LC/MS (ESI+): tr = 11.73 min, m/z $[M+H]^+$ = 831.49. UV purity: 99% (254 nm). HRMS (Maldi-TOF): m/z calculated for $[M+H]^+$ = 831.4180; found for $[M+H]^+$ = 831.4204. ^{1}H NMR (300 MHz, $CDCl_3$): δ -0.11 (d, *J* = 7.1 Hz, 3H), 0.57 (d, *J* = 6.8 Hz, 3H), 0.81 (d, *J* = 6.9 Hz, 3H), 0.86 (d, *J* = 6.1 Hz, 2H), 1.00 (d, *J* = 7.0 Hz, 3H), 1.32-1.56 (m, 4H), 1.64-1.80 (m, 3H), 1.71 (s, 3H), 1.97 (s, 3H), 2.00 (s, 3H), 2.28-2.38 (m, 1H), 2.29 (s, 3H), 2.53-2.66 (m, 1H), 2.91-3.23 (m, 3H), 3.04 (s, 3H), 3.30 (dd, *J* = 7.0, 2.1 Hz, 1H), 3.45 (s, 1H), 3.51-3.88 (m, 6H), 4.75 (d, *J* = 10.5 Hz, 1H), 5.07 (dd, *J* = 12.5, 7.1 Hz, 1H), 5.95 (dd, *J* = 15.5, 6.7 Hz, 1H), 6.10 (dd, *J* = 12.5, 0.8 Hz, 1H), 6.22 (dd, *J* = 10.3, 1.2 Hz, 1H), 6.33 (dd, *J* = 15.5, 10.3 Hz, 1H), 8.19 (s, 1H), 8.64 (s, 1H), 14.45 (s, 1H). ^{13}C NMR (75 MHz, $CDCl_3$): δ 4.66, 4.73, 7.7, 8.8, 10.6, 11.2, 17.4, 20.3, 21.0, 21.8, 33.0, 34.0, 37.6, 37.7, 38.3, 40.1, 52.0, 57.0, 72.7, 73.0, 76.9, 80.4, 91.5, 105.5, 107.4, 108.8, 111.7, 114.9, 115.5, 124.2, 125.7, 130.9, 133.4, 141.0, 141.6, 144.0, 156.5, 168.1, 168.3, 171.6, 172.2, 182.0, 193.0.

Compound 23 : the title compound was obtained as a purple solid (yield = 59%) following the general procedure and using 1-cyclopentylpiperidin-4-one as ketone. LC/MS (ESI+): tr = 11.65 min, m/z $[M+H]^+$ = 859.40. UV purity: 99% (254 nm). HRMS (Maldi-TOF): m/z calculated for $[M+H]^+$ = 859.4493; found for $[M+H]^+$ = 859.4489. ^{1}H NMR (300 MHz, $CDCl_3$): δ -0.14 (d, *J* = 6.9 Hz, 3H), 0.56 (d, *J* = 6.7 Hz, 3H), 0.81 (d, *J* = 6.8 Hz, 3H), 0.99 (d, *J* = 6.8 Hz, 3H), 1.32_1.48 (m, 2H), 1.57-1.78 (m, 5H), 1.71 (s, 3H), 1.79-2.42 (m, 7H), 1.97 (s, 3H), 1.99 (s, 3H), 2.28 (s, 3H), 2.95-3.03 (m, 1H), 3.04 (s, 3H), 3.07-3.79 (m, 11H), 4.78 (d, *J* = 10.4, 1H), 5.05 (dd, *J* = 12.5, 6.7 Hz, 1H), 5.95 (dd, *J* = 15.5, 6.7 Hz, 1H), 6.07 (d, *J* = 12.5 Hz, 1H), 6.21 (d, *J* = 10.3 Hz, 1H), 6.33 (dd, *J* = 15.5, 10.3 Hz, 1H), 8.30 (s, 1H), 8.69 (s, 1H), 14.50 (s, 1H). ^{13}C NMR (75 MHz, $CDCl_3$): δ 7.6, 8.8, 10.4, 11.1, 17.4, 20.4, 21.0, 21.7, 23.8, 28.8, 32.7, 33.0, 33.7, 37.6, 37.7, 38.2, 50.2, 50.3, 57.0 68.4, 72.7, 73.1, 76.9, 80.1, 91.0, 105.4, 107.3, 108.7, 111.7, 114.9, 115.5, 124.3, 124.7, 130.9, 133.3, 140.8, 141.8, 143.6, 156.6, 168.2, 168.3, 171.7, 172.2, 182.2, 193.1.

Compound 24 : the title compound was obtained as a purple solid (yield = 75%) following the general procedure and using 1-(cyclohexylmethyl)piperidin-4-one as ketone. LC/MS (ESI+): tr = 12.78 min, m/z $[M+H]^+$ = 887.69. UV purity: 99% (254 nm). HRMS (Maldi-TOF): m/z calculated for $[M+H]^+$ =

887.4806; found for $[M+H]^+$ = 887.4811. ^{1}H NMR (300 MHz, $CDCl_3$): δ -0.13 (d, *J* = 7.0 Hz, 3H), 0.57 (d, *J* = 6.6 Hz, 3H), 0.82 (d, *J* = 6.2 Hz, 3H), 0.99 (d, *J* = 6.9 Hz, 3H), 1.06-1.46 (m, 7H), 1.60-1.84 (m, 6H), 1.71 (s, 3H), 1.86-2.10 (m, 3H), 1.97 (s, 3H), 1.99 (s, 3H), 2.20-2.40 (m, 1H), 2.29 (s, 3H), 2.89-3.02 (m, 3H), 3.04 (s, 3H), 3.30 (s, 3H), 3.38-3.72 (m, 7H), 4.76 (d, *J* = 10.3 Hz, 1H), 5.06 (dd, J = 12.5, 7.0 Hz, 1H), 5.95 (dd, *J* = 15.5, 6.6 Hz, 1H), 6.08 (d, J = 12.5 Hz, 1H), 6.21 (d, *J* = 10.0 Hz, 1H), 6.34 (dd, *J* = 15.5, 10.3 Hz, 1H), 8.18 (s, 1H), 8.67 (brs, 1H), 14.47 (s, 1H). ^{13}C NMR (75 MHz, $CDCl_3$): δ 7.6, 8.8, 10.3, 11.1, 17.4, 20.4, 21.0, 21.6, 25.6, 25.8, 29.7, 31.7, 32.6, 33.0, 33.5, 37.6, 37.8, 38.2, 51.6, 57.0, 63.9, 72.8, 73.2, 76.9, 79.9, 91.1, 105.3, 108.7, 111.8, 114.9, 115.5, 124.4, 124.8, 130.9, 133.3, 140.7, 142.0, 143.5, 156.7, 168.2, 168.3, 171.7, 172.3, 182.3, 193.1.

Compound 27 : the title compound was obtained as a purple solid (yield = 42%) following the general procedure and using 1-methylpiperidin-4-one as ketone. LC/MS (ESI+): tr = 10.62 min, m/z $[M+H]^+$ = 805.40. UV purity: 99 % (254 nm). HRMS (Maldi-TOF): m/z calculated for $[M+H]^+$ = 805.4024; found for $[M+H]^+$ = 805.4019. ^{1}H NMR (300 MHz, $CDCl_3$): δ -0.11 (d, *J* = 7.1 Hz, 3H), 0.57 (d, *J* = 6.8 Hz, 3H), 0.82 (d, *J* = 6.9 Hz, 3H), 1.00 (d, *J* = 7.0 Hz, 3H), 1.31-1.50 (m, 2H), 1.63-1.80 (m, 3H), 1.74 (s, 3H), 1.97 (s, 3H), 2.00 (s, 3H), 2.27-2.38 (m, 1H), 2.30 (s, 3H), 2.91-3.01 (m, 1H), 2.95 (s, 3H), 3.05 (s, 3H), 3.07-3.25 (m, 2H), 3.30 (dd, *J* = 7.1, 2.2 Hz, 1H), 3.38-3.85 (m, 7H), 4.74 (d, *J* = 10.6 Hz, 1H), 5.06 (dd, *J* = 12.5, 7.1 Hz, 1H), 5.95 (dd, J = 15.6, 6.7 Hz, 1H), 6.11 (d, *J* = 12.5 Hz, 1H), 6.23 (dd, *J* = 10.2, 1.1 Hz, 1H), 6.35 (dd, *J* = 15.6, 10.2 Hz, 1H), 8.11 (s, 1H), 8.66 (s, 1H), 14.40 (s, 1H). ^{13}C NMR (75 MHz, $CDCl_3$): δ 7.7, 8.8, 10.7, 11.2, 17.4, 20.3, 21.0, 21.8, 33.0, 33.1, 34.1, 37.6, 37.7, 38.4, 43.7, 52.8, 57.0, 72.7, 73.0, 76.9, 80.5, 90.4, 105.8, 107.5, 108.9, 111.6, 115.1, 115.3, 124.3, 124.6, 130.8, 133.5, 141.0, 141.5, 144.1, 156.7, 168.1, 168.4, 171.6, 172.3, 182.1, 193.0.

Compound 28 : the title compound was obtained as a purple solid (yield = 23%) following the general procedure and using 1-ethylpiperidin-4-one as ketone. LC/MS (ESI+): tr = 10.98 min, m/z $[M+H]^+$ = 819.33. UV purity: 96% (254 nm). HRMS (Maldi-TOF): m/z calculated for $[M+H]^+$ = 819.4180; found for $[M+H]^+$ = 819.4184. ^{1}H NMR (300 MHz, $CDCl_3$): δ -0.10 (d, *J* = 7.1Hz, 3H), 0.59 (d, *J* = 6.8 Hz, 3H), 0.84 (d, *J* = 6.9 Hz, 3H), 1.00 (d, *J* = 7.0 Hz, 3H), 1.35-1.42 (m, 2H), 1.56 (t, *J* = 10.3 Hz, 3H), 1.67-1.82 (m, 3H), 1.72 (s, 3H), 1.99 (s, 3H), 2.01 (s, 3H), 2.26-2.40 (m, 1H), 2.31 (s, 3H), 2.94-3.02 (m, 1H), 3.06 (s, 3H), 3.13-3.35 (m, 5H), 3.42-3.76 (m, 7H), 4.76 (d, *J* = 9.9 Hz, 1H), 5.07 (dd, *J* = 12.5, 7.1 Hz, 1H), 5.97 (dd, J = 15.5, 6.7 Hz, 1H), 6.1 (d, J = 12.5 Hz, 1H), 6.2 (dd, *J* = 10.3, 1.0 Hz, 1H), 6.36 (dd, *J* = 15.5, 10.3 Hz), 8.19 (s, 1H), 8.63 (brs, 1H), 14.42 (s, 1H). ^{13}C NMR (75 MHz, $CDCl_3$): δ 7.7, 8.8, 9.7, 10.6, 11.2, 17.4, 20.4, 21.0, 21.8, 32.9, 33.0, 34.0, 37.6 , 38.4, 50.2, 50.3, 52.3, 57.0, 72.7, 73.1, 77.0, 80.5, 91.0, 105.7, 107.5, 108.9, 111.7, 115.1, 115.4, 124.3, 124.7, 130.9, 133.5, 141.0, 141.5, 144.0, 156.7, 168.2, 168.4, 171.7, 172.3, 182.2, 193.1.

Compound 29 : the title compound was obtained as a purple solid (yield = 49%) following the general procedure and using 1-propylpiperidin-4-one as ketone. LC/MS (ESI+): tr = 11.42 min, m/z $[M+H]^+$ = 833.32. UV purity: 99% (254 nm). HRMS (Maldi-TOF): m/z calculated for $[M+H]^+$ = 833.4337; found for $[M+H]^+$ = 833.4342. ^{1}H NMR (300 MHz, $CDCl_3$): δ -0.11 (d, *J* = 7.1 Hz, 3H), 0.59 (d, *J* = 6.8 Hz, 3H), 0.83 (d, *J* = 6.9 Hz, 3H), 1.01 (d, *J* = 7.0 Hz, 3H), 1.06 (t, *J* = 7.4 Hz, 3H), 1.33-1.49 (m, 2H), 1.64-1.80 (3H), 1.72 (s, 3H), 1.97-2.07 (m, 2H), 1.98 (s, 3H), 2.01 (s, 3H), 2.28-2.38 (m, 1H), 2.31 (s, 3H), 2.94-3.02 (m, 1H), 3.04-3.14 (m, 2H), 3.06 (s, 3H), 3.15-3.37 (m, 3H), 3.43 (s, 1H), 3.48-3.76 (m, 6H), 4.76 (dd, *J* = 10.6, 1.2 Hz, 1H), 5.07 (dd, *J* = 12.5, 7.1 Hz, 1H), 5.97 (dd, *J* = 15.6, 6.7 Hz, 1H), 6.11 (d, *J* = 12.5 Hz, 1H), 6.24 (dd, *J* = 10.3, 1.2 Hz, 1H), 6.36 (dd, J = 15.6, 10.3 Hz, 1H), 8.1 (s, 1H), 8.6 (s, 1H), 14.41 (s, 1H). ^{13}C NMR (75 MHz, $CDCl_3$): δ 7.7, 8.8, 10.6, 11.2, 11.3, 17.4, 17.7, 20.4, 21.0, 21.8, 32.9, 33.0,

33.9, 37.6, 38.4, 50.8, 57.0, 59.1, 72.7, 73.1, 76.9, 80.5, 90.9, 105.7, 107.5, 108.8, 111.7, 115.1, 115.4, 124.3, 124.7, 130.9, 133.5, 141.0, 141.5, 144.0, 156.7, 168.2, 168.4, 171.7, 172.3, 182.2, 193.1.

Compound 30 : the title compound was obtained as a purple solid (yield = 49%) following the general procedure and using 1-butylpiperidin-4-one as ketone. LC/MS (ESI+): tr = 11.87 min, m/z $[M+H]^+$ = 847.40. UV purity: 99% (254 nm). HRMS (Maldi-TOF): m/z calculated for $[M+H]^+$ = 847.4493; found for $[M+H]^+$ = 847.4492. ^{1}H NMR (300 MHz, $CDCl_3$): δ -0.13 (d, *J* = 7.1 Hz, 3H), 0.57 (d, *J* = 6.9 Hz, 3H), 0.82 (d, *J* = 6.9 Hz, 3H), 0.98 (t, *J* = 7.3 Hz, 3H), 1.00 (d, *J* = 7.0 Hz, 3H), 1.30-1.49 (m, 4H), 1.63-1.79 (m, 3H), 1.71 (s, 3H), 1.85-2.01 (m, 2H), 1.97 (s, 3H), 1.99 (s, 3H), 2.26-2.38 (m, 1H), 2.29 (s, 3H), 2.99-3.01 (m, 1H), 3.04 (s, 3H), 3.06-3.33 (m, 5H), 3.45 (s, 1H), 3.47-3.73 (m, 6H), 4.75 (dd, *J* = 10.47, 1.05 Hz, 1H), 5.05 (dd, *J* = 12.6, 7.2 Hz, 1H), 5.95 (dd, *J* = 15.6, 6.7 Hz, 1H), 6.09 (dd, *J* = 12.6, 0.8 Hz, 1H), 6.22 (dd, *J* = 10.3, 1.2 Hz, 1H), 6.34 (dd, *J* = 15.6, 10.3 Hz, 1H), 8.13 (s, 1H), 8.63 (brs, 1H), 14.43 (s, 1H). ^{13}C NMR (75 MHz, $CDCl_3$): δ 7.7, 8.8, 10.5, 11.2, 13.6, 17.4, 20.3, 20.4, 21.0, 21.7, 26.0, 32.8, 33.0, 33.9, 37.6, 38.3, 50.8, 57.0, 57.4, 72.7, 73.0, 76.9, 80.3, 91.0, 105.6, 107.4, 108.8, 111.6, 115.0, 115.4, 124.2, 124.7, 130.8, 133.4, 140.9, 141.6, 143.9, 156.6, 168.1, 168.3, 171.6, 172.2, 182.1, 193.1.

Compound 31 : the title compound was obtained as a purple solid (yield = 61%) following the general procedure and using 1-isopropylpiperidin-4-one as ketone. LC/MS (ESI+): tr = 11.15 min, m/z $[M+H]^+$ = 833.42. UV purity: 99% (254 nm). HRMS (Maldi-TOF): m/z calculated for $[M+H]^+$ = 833.4337; found for $[M+H]^+$ = 833.4353. ^{1}H NMR (300 MHz, $CDCl_3$): δ -0.12 (d, *J* = 7.1 Hz, 3H), 0.58 (d, *J* = 6.8 Hz, 3H), 0.83 (d, *J* = 6.9 Hz, 3H), 1.00 (d, *J* = 7.0 Hz, 3H), 1.33-1.47 (m, 2H), 1.57 (d, *J* = 5.6 Hz, 6H), 1.65-1.80 (m, 3H), 1.71 (s, 3H), 1.98 (s, 3H), 2.01 (s, 3H), 2.30 (s, 3H), 2.31-2.39 (m, 1H), 2.94-3.02 (m, 1H), 3.05 (s, 3H), 3.20-3.40 (m, 3H), 3.43 (s, 1H), 3.45-3.72 (m, 6H), 3.71-2.92 (m, 1H), 4.77 (dd, *J* = 10.6, 1.2 Hz, 1H), 5.07 (dd, *J* = 12.5, 7.0 Hz, 1H), 5.97 (dd, *J* = 15.6, 6.7 Hz, 1H), 6.08 (dd, *J* = 12.3, 0.7 Hz, 1H), 6.23 (dd, *J* = 10.3, 1.2 Hz, 1H), 6.35 (dd, *J* = 15.6, 10.5 Hz, 1H), 8.1 (s, 1H), 8.6 (brs, 1H), 14.38 (s, 1H). ^{13}C NMR (75 MHz, $CDCl_3$): δ 7.6, 8.7, 10.5, 11.1, 17.0, 17.1, 17.3, 20.2, 20.9, 31.7, 32.7, 32.9, 33.8, 37.5, 37.6, 38.3, 46.2, 46.5, 56.9, 57.9, 72.6, 73.0, 76.8, 80.3, 91.0, 105.6, 107.3, 108.8, 111.5, 114.9, 115.4, 124.1, 124.5, 130.7, 133.43, 140.9, 141.4, 143.8, 156.4, 167.9, 168.2, 171.5, 172.1, 182.0, 192.6.

Compound 32 : the title compound was obtained as a purple solid (yield = 67%) following the general procedure and using 1-isopentylpiperidin-4-one as ketone. LC/MS (ESI+): tr = 12.38 min, m/z $[M+H]^+$ = 861.51. UV purity: 99% (254 nm). HRMS (Maldi-TOF): m/z calculated for $[M+H]^+$ = 861.4650; found for $[M+H]^+$ = 861.4656. ^{1}H NMR (300 MHz, $CDCl_3$): δ -0.14 (d, *J* = 7.1 Hz, 3H), 0.55 (d, *J* = 6.8 Hz, 3H), 0.81 (d, *J* = 6.8 Hz, 3H), 0.92-1.01 (m, 9H), 1.31-1.41 (m, 2H), 1.59-1.78 (m, 4H), 1.70 (s, 3H), 1.79-1.91 (m, 2H), 1.96 (s, 3H), 1.98 (s, 3H), 2.24-2.39 (m, 1H), 2.27 (s, 3H), 2.91-3.38 (m, 6 H), 3.03 (s, 3H), 3.39-3.79 (m, 7H), 4.75 (d, *J* = 10.3 Hz, 1H), 5.04 (dd, *J* = 12.5, 7.0 Hz, 1H), 5.94 (dd, *J* = 15.5, 6.7 Hz, 1H), 6.07 (dd, *J* = 12.5, 0.6 Hz, 1H), 6.21 (d, *J* = 10.0 Hz, 1H), 6.33 (dd, *J* = 15.5, 10.3 Hz, 1H), 8.1 (s, 1H), 8.6 (brs, 1H), 14.43 (s, 1H). ^{13}C NMR (75 MHz, $CDCl_3$): δ 7.6, 8.8, 10.5, 11.1, 17.3, 20.3, 21.0, 21.7, 22.3, 22.4, 26.5, 32.4, 32.8, 32.9, 33.8, 37.5, 37.6, 38.3, 50.7, 50.8, 56.2, 57.0, 72.7, 73.0, 76.8, 80.3, 91.0, 105.5, 107.3, 108.7, 111.6, 114.9, 115.4, 124.2, 124.6, 130.8, 133.4, 140.9, 141.6, 143.8, 156.6, 168.1, 168.2, 171.6, 172.2, 182.1, 193.1.

Compound 33 : the title compound was obtained as a purple solid (yield = 48%) following the general procedure and using 1-tert-butylpiperidin-4-one as ketone. LC/MS (ESI+): tr = 11.37 min, m/z $[M+H]^+$ = 847.40. UV purity: 99% (254 nm). HRMS (Maldi-TOF): m/z calculated for $[M+H]^+$ = 847.4493; found for $[M+H]^+$ = 847.4484. ^{1}H NMR (300 MHz, $CDCl_3$): δ -0.13 (d, *J* = 7.1 Hz, 3H), 0.58 (d, *J* = 6.8 Hz, 3H),

0.82 (d, *J* = 6.9 Hz, 3H), 1.00 (d, *J* = 6.9 Hz, 3H), 1.06 (t, *J* = 7.4 Hz, 3H), 1.3-1.56 (m, 2H), 1.58-1.80 (m, 3H), 1.63 (s, 9H), 1.79 (s, 3H), 2.28-2.39 (m, 1H), 2.28 (s, 3H), 2.94-3.25 (m, 1H), 3.05 (s, 3H), 3.27-3.50 (m, 3H), 3.56-3.91 (m, 7H), 4.80 (d, *J* = 10.3 Hz, 1H), 5.06 (dd, *J* = 12.5, 6.7 Hz, 1H), 5 .98 (dd, *J* = 15.5 Hz, 6.7 Hz, 1H), 6.09 (d, *J* = 12.5, 1H), 6.23 (d, *J* = 10.3 Hz, 1H), 6.35 (dd, *J* = 15.5, 10.3 Hz, 1H), 8.20 (s, 1H), 8.6 (s, 1H),14 .46 (s, 1H). ^{13}C NMR (75 MHz, $CDCl_3$): δ 7.6, 8.7, 10.2, 11.1, 17.3, 20.3, 20.9, 21.6, 25.0, 32.7, 32.9, 33.8, 37.5, 37.7, 38.1, 44 .7, 57.0 (2C), 63.4, 72.7, 73.0, 76.8, 79.9, 91.0, 105.3, 107.2, 108.7, 111.6, 114.8, 115.5, 124.2, 124.6, 130.7, 133.3, 140.8, 141.7, 143.5, 156.5, 168.0, 168.2, 171.6, 172.1, 182.1, 192.6.

Compound 34 : the title compound was obtained as a purple solid (yield = 61%) following the general procedure and using 1-(2,2-dimethylpropyl)piperidin-4-one as ketone. LC/MS (ESI+): tr = 12.05 min, m/z $[M+H]^+$ = 861.42. UV purity: 98% (254 nm). HRMS (Maldi-TOF): m/z calculated for $[M+H]^+$ = 861.4650; found for $[M+H]^+$ = 861.4637. ^{1}H NMR (300 MHz, $CDCl_3$): δ -0.13 (d, *J* = 7.1 Hz, 3H), 0.56 (d, *J* = 6.8 Hz, 3H), 0.82 (d, *J* = 6.9 Hz, 3H), 0.99 (d, *J* = 7.0 Hz, 3H), 1.19-1.28 (s, 9H), 1.35-1.50 (m, 2H), 1.61-1.79 (m, 3H), 1.72 (s, 3H), 2.20-2.39 (m, 1H), 2.28 (s, 1H), 2.67-3.12 (4H), 3.04 (s, 3H), 3.31 (dd, *J* = 6.7, 1.8 Hz, 1H), 3.36-3.94 (m, 8H), 4.79 (d, *J* = 9.7 Hz, 1H), 5.05 (dd, *J* = 12.5, 6.7 Hz, 1H), 5.59 (dd, *J* = 15.5, 6.7 Hz, 1H), 6.08 (dd, *J* = 12.5, 0.7 Hz, 1H), 6.21 (dd, *J* = 10.3, 1.0 Hz, 1H), 6.33 (dd, *J* = 15.5, 10.3 Hz, 1H), 8.25 (s, 1H), 8.71 (brs, 1H), 14.55 (s, 1H) . ^{13}C NMR (75 MHz, $CDCl_3$): δ 7.6, 8.8, 10.4, 11.1, 17.4, 20.4, 21.0, 21.7, 28.5, 32.4, 33.0, 33.9, 37.6, 37.7, 38.2, 54.7, 54.9, 57.0, 71.8, 72.7, 73.1, 76.9, 80.0, 91.1, 105.3, 107.3, 108.7, 111.8, 114.8, 115.6, 124.3, 124.8, 130.9, 133.3, 140.8, 142.0, 143.6, 156.4, 168.2, 168.3, 171.6, 172.2, 182.1, 193.1.

Compound 35 : the title compound was obtained as a purple solid (yield = 72%) following the general procedure and using 1-(3,3-dimethylbutyl)piperidin-4-one as ketone. LC/MS (ESI+): tr = 12.88 min, m/z $[M+H]^+$ = 875.56. UV purity: 99% (254 nm). HRMS (Maldi-TOF): m/z calculated for $[M+H]^+$ = 875.4806; found for $[M+H]^+$ = 875.4819. ^{1}H NMR (300 MHz, $CDCl_3$): δ -0.13 (d, *J* = 7.0 Hz, 3H), 0.56 (d, *J* = 6.8 Hz, 3H), 0.82 (d, *J* = 6.9 Hz, 3H), 0.92-1.05 (m, 12H), 1.33-1.48 (m, 2H), 1.61-1.80 (3H), 1.67 (s, 3H), 1.81-1.93 (m, 2H), 1.97 (s, 3H), 1.99 (s, 3H), 2.22-2.38 (m, 1H), 2.28 (s, 3H), 2.92-3.36 (m, 6H), 3.04 (s, 3H), 3.41-3.75 (m, 7H), 4.76 (d, *J* = 10.2 Hz, 1H), 5.05 (dd, *J* = 12.5, 6.8 Hz, 1H), 5.95 (dd, *J* = 15.5, 6.7 Hz, 1H), 6.08 (d, *J* = 12.5 Hz, 1H), 6.22 (d, *J* = 10.2, 1H), 6.32 (dd, *J* = 15.5, 10.2 Hz, 1H), 8.24 (s, 1H), 8.63 (brs, 1H), 14.45 (s, 1H). ^{13}C NMR (75 MHz, $CDCl_3$): δ 7.7, 8.8, 10.5, 11.2, 17.4, 20.3, 21.0, 21.7, 29.2, 30.0, 32.8, 33.0, 33.9, 37.0, 37.6, 37.7, 38.3, 50.7, 50.9, 54.3, 57.0, 72.7, 73.1, 76.9, 80.2, 91.0, 105.5, 107.3, 108.7, 111.7, 115.0, 115.4, 124.2, 124.7, 130.8, 133.3, 140.9, 141.7, 143.7, 156.6, 168.2, 168.3, 171.6, 172.2, 182.1, 193.1.

Compound 36 : the title compound was obtained as a purple solid (yield = 67%) following the general procedure and using 1-(cyclopropylmethyl)piperidin-4-one as ketone. LC/MS (ESI+): tr = 11.33 min, m/z $[M+H]^+$ = 845.42. UV purity: 99% (254 nm). HRMS (Maldi-TOF): m/z calculated for $[M+H]^+$ = 845.4337; found for $[M+H]^+$ = 845.4365. ^{1}H NMR (300 MHz, $CDCl_3$): δ -0.13 (d, *J* = 7.1 Hz, 3H), 0.44-0.54 (m, 2H), 0.58 (d, *J* = 6.8 Hz, 3H), 0.74-0.86 (m, 5H), 0.99 (d, *J* = 7.0 Hz, 3H), 1.30-1.49 (m, 3H), 1.97 (s, 3H), 2.00 (s, 3H), 2.18-2.41 (m, 1H), 2.29 (s, 3H), 2.88-2.35 (m, 6H), 3.04 (s, 3H), 3.37-3.86 (m, 7H), 4.77 (d, *J* = 10.5 Hz, 1H), 5.05 (dd, *J* = 12.5, 6.9 Hz, 1H), 5.95 (dd, *J* = 15.6, 6.8 Hz, 1H), 6.08 (dd, *J* = 12.5, 0.7 Hz, 1H), 6.22 (dd, *J* = 10.3, 1.1 Hz, 1H), 6.34 (dd, *J* = 15.6, 10.3 Hz, 1H), 8.30 (s, 1H), 8.78 (s, 1H), 14.50 (s, 1H). ^{13}C NMR (75 MHz, $CDCl_3$): δ 4.9, 5.1, 5.9, 7.7, 8.8, 10.5, 11.2, 17.4, 20.4, 21.0, 21.7, 32 .8, 33.0, 33.8, 37.6, 37.7, 38.3, 50.4, 50.6, 57 .0, 61.9, 72.7, 73.1, 76.9, 80.2, 91.1, 105.4, 107.3,

108.8, 111.7, 114.9, 115.5, 124.3, 124.7, 130.9, 133.3, 140.8, 141.8, 143.7, 156.6, 168.2, 168.3, 171.6, 172.2, 182.2, 193.0.

Compound 37 : the title compound was obtained as a purple solid (yield = 60%) following the general procedure and using 1-(cyclopentylmethyl)piperidin-4-one as ketone. LC/MS (ESI+): tr = 12.25 min, m/z $[M+H]^+$ = 873.58. UV purity: 99% (254 nm). HRMS (Maldi-TOF): m/z calculated for $[M+H]^+$ = 873.4650; found for $[M+H]^+$ = 873.4651. ^{1}H NMR (300 MHz, $CDCl_3$): δ -0.13 (d, *J* = 7.1 Hz, 3H), 0.57 (d, *J* = 7.4 Hz, 3H), 0.83 (d, *J* = 6.9 Hz, 3H), 1.00 (d, *J* = 7.0 Hz, 3H), 1.33-1.48 (m, 4H), 1.55_1.80 (m, 7H), 1.69 (s, 3H), 1.93-2.09 (m, 2H), 1.98 (s, 3H), 2.00 (s, 3H), 2.12-2.56 (m, 2H), 2.23 (s, 3H), 2.92-3.01 (m, 1H), 3.05 (s, 3H), 3.08-3.78 (m, 12H), 4.79 (d, *J* = 10.5 Hz, 1H), 5.06 (dd, *J* = 12.5, 6.7 Hz, 1H), 5.96 (dd, *J* = 15.5, 6.7 Hz, 1H), 6.08 (dd, *J* = 12.5, 0.6 Hz, 1H), 6.22 (dd, *J* = 10.3, 1.0 Hz, 1H), 6.34 (dd, *J* = 15.5, 10.3 Hz, 1H), 8.33 (s, 1H), 8.71 (s, 1H), 14.53 (s, 1H). ^{13}C NMR (75 MHz, $CDCl_3$): δ 7.7, 8.8, 10.4, 11.2, 17.4, 20.4, 21.0, 21.7, 25.1, 25.2, 32.1, 32.2, 32.7, 33.0, 33.7, 35.5, 37.6, 37.7, 38.2, 51.2, 51.4, 57.1, 62.9, 72.7, 73.1, 76.9, 80.0, 91.1, 105.4, 107.3, 108.7, 111.8, 114.9, 115.5, 124.3, 124.8, 130.9, 133.3, 140.8, 141.9, 143.6, 156.6, 168.2, 171.7, 172.3, 182.2, 193.1.

Compound 38 : the title compound was obtained as a purple solid (yield = 65%) following the general procedure and using 1-cyclohexylpiperidin-4-one as ketone. LC/MS (ESI+): tr = 11.97 min, m/z $[M+H]^+$ = 873.45. UV purity: 99% (254 nm). HRMS (Maldi-TOF): m/z calculated for $[M+H]^+$ = 873.4650; found for $[M+H]^+$ = 873.4655. ^{1}H NMR (300 MHz, $CDCl_3$): δ -0.15 (d, *J* = 7.1 Hz, 3H), 0.59 (d, *J* = 6.8 Hz, 3H), 0.83 (d, *J* = 6.9 Hz, 3H), 0.99 (d, *J* = 7.0 Hz, 3H), 1.17-2.05 (m, 13H), 1.71 (s, 3H), 1.98 (s, 3H), 1.99 (s, 3H), 2.13-2.53 (m, 3H), 2.28 (s, 3H), 2.93-3.01 (m, 1H), 3.04 (s, 3H), 3.08-3.91 (m, 11H), 4.43 (d, *J* = 10.3 Hz, 1H), 5.04 (dd, J = 12.5, 6.5 Hz, 1H), 5.97 (dd, *J* = 15.6, 6.7 Hz, 1H), 6.05 (dd, *J* = 12.5, 0.7 Hz, 1H), 6.2 (dd, *J* = 10.2, 1.0 Hz, 1H), 6.35 (dd, *J* = 15.6, 10.3 Hz, 1H), 8.31 (s, 1H), 8.70 (brs, 1H), 14.51 (s, 1H). ^{13}C NMR (75 MHz, $CDCl_3$): δ 7.7, 8.8, 10.2, 11.1, 17.4, 20.4, 21.0, 21.6, 25.1, 25.2, 25.3, 27.0, 27.1 , 32.6, 33 .0, 33.8, 37.5, 37.8, 38.2, 47.0, 47.2, 57.1, 66.1, 72.7, 73.2, 76.9, 79.7, 91.2, 105.3, 107.2, 108.7, 111.7, 114.8, 115.6, 124.4, 124.7, 130.8, 133.4, 140.8, 141.9, 143.4, 156.6, 168.1, 168.2, 171.7, 172.2, 182.2, 192.2.

Compound 39 : the title compound was obtained as a purple solid (yield = 38%) following the general procedure and using 1-phenylpiperidin-4-one as ketone. LC/MS (ESI+): tr = 11.21 min, m/z $[M+H]^+$ = 867.53. UV purity: 97% (254 nm). HRMS (Maldi-TOF): m/z calculated for $[M+H]^+$ = 867.4180; found for $[M+H]^+$ = 867.4177. ^{1}H NMR (300 MHz, $CDCl_3$): δ -0.04 (d, *J* = 7.1 Hz, 3H), 0.61 (d, *J* = 6.9 Hz, 3H), 0.83 (d, *J* = 6.9 Hz, 3H), 1.03 (d, *J* = 7.0 Hz, 3H), 1.38-1.51 (m, 1H), 1.69-1.89 (m, 3H), 1.73 (s, 3H), 1.98-2.20 (m, 3H), 2.00 (s, 3H), 2.03 (s, 3H), 2.32 (s, 3H), 2.33-2.43 (m, 1H), 2.95- 3.03 (m, 1H), 3.04 (s, 3H), 3.33 (dd, J = 7.3, 2.1 Hz, 1H), 3.48 (s, 1H), 3.52-3.85 (m, 6H), 4.76 (dd, *J* = 10.5, 1.2 Hz, 1H), 5.12 (dd, *J* = 12.5, 7.3 Hz, 1H), 5.99 (dd, *J* = 15.6, 6.6 Hz, 1H), 6.16 (dd, *J* = 12.5, 0.8 Hz, 1H), 6.24 (dd, *J* = 10.3, 1.3 Hz, 1H), 6.36 (dd, *J* = 15.6, 10.3 Hz, 1H), 6.88 (t, *J* = 7.3 Hz, 1H), 6.99-7.05 (m, 2H), 7.25-7.33 (m, 2H), 8.27 (s, 1H), 8.98 (s, 1H), 14.65 (s, 1H). ^{13}C NMR (75 MHz, $CDCl_3$): δ 7.7, 8.8, 11.0, 11.3, 17.5, 20.3, 21.1, 21.9, 33.1, 35.0, 35.9, 37.7, 37.8, 38.3, 47.4, 47.6, 56.9, 72.6, 73.2, 76.9, 80.8, 94.3, 104.9, 107.4, 109.0, 111.8, 114.5, 115.6, 116.7, 119.9, 124.1, 125.1, 129.3, 131.1, 133.2, 141.1, 142.0, 144.3, 150.6, 155.6, 168.2, 168.6, 171.6, 172.3, 181.4, 192.6.

Compound 40 : the title compound was obtained as a purple solid (yield = 68%) following the general procedure and using 1-benzylpiperidin-4-one as ketone. LC/MS (ESI+): tr = 12.29 min, m/z $[M+H]^+$ = 881.58. UV purity: 99% (254 nm). HRMS (Maldi-TOF): m/z calculated for $[M+H]^+$ = 881.4337; found

for $[M+H]^+$ = 881.4338. ^{1}H NMR (300 MHz, $CDCl_3$): δ -0.13 (d, *J* = 7.1 Hz, 3H), 0.56 (d, *J* = 6.8 Hz, 3H), 0.82 (d, *J* = 6.9 Hz, 3H), 1.00 (d, *J* = 7.0 Hz, 3H), 1.36-1.49 (m, 2H), 1.61-1.78 (m, 3H), 1.74 (s, 3H), 1.98 (s, 3H), 1.99 (s, 3H), 2.26-2.32 (m, 1H), 2.29 (s, 3H), 2.93-3.20 (m, 3H), 3.05 (s, 3H), 3.30-3.70 (m, 8H), 4.22 (d, *J* = 12.9 Hz, 1H), 4.30 (d, *J* = 12.9 Hz, 1H), 4.79 (d, *J* = 10.5, 1H), 5.07 (dd, *J* = 12.5, 6.7 Hz, 1H), 5.96 (dd, *J* = 15.6, 6.8 Hz, 1H), 6.09 (dd, *J* = 12.5, 0.8 Hz, 1H), 6.21 (dd, *J* = 10.3, 1.1 Hz, 1H), 6.34 (dd, *J* = 15.6, 10.3 Hz, 1H), 7.37-7.51 (m, 3H), 7.69-7.78 (m, 2H), 8.34 (s, 1H), 8.73 (brs, 1H), 14.53 (s, 1H). ^{13}C NMR (75 MHz, $CDCl_3$): δ 7.7, 8.8, 10.4, 11.1, 17.4, 20.4, 21.0, 21.7, 32.9, 33.0, 33.9, 37.6, 37.7, 38.2, 50.6, 50.9, 57.1, 61.3, 72.7, 73.2, 76.9, 80.0, 91.4, 105.3, 107.3, 107.7, 108.7, 111.8, 114.9, 115.6, 124.3, 124.8, 129.3, 129.9, 130.9, 131.2, 133.3, 140.8, 141.9, 143.6, 156.5, 168.2, 168.3, 171.7, 172.3, 182.2, 193.1.

Compound 41: the title compound was obtained as a purple solid (yield = 78%) following the general procedure and using 1-(2-phenylethyl)piperidin-4-one as ketone. LC/MS (ESI+): tr = 12.70 min, m/z $[M+H]^+$ = 895.60. UV purity: 99% (254 nm). HRMS (Maldi-TOF): m/z calculated for $[M+H]^+$ = 895.4493; found for $[M+H]^+$ = 895.4506. ^{1}H NMR (300 MHz, $CDCl_3$): δ -0.12 (d, *J* = 7.0 Hz, 3H), 0.58 (d, *J* = 6.8 Hz, 3H), 0.83 (d, *J* = 6.9 Hz, 3H), 0.99 (d, *J* = 7.0 Hz, 3H), 1.37-1.49 (m, 2H), 1.60-1.80 (m, 3H), 1.72 (s, 3H), 1.98 (s, 3H), 1.99 (s, 3H), 2.24-2.39 (m, 1H), 2.29 (s, 3H), 2.94-3.02 (m, 1H), 3.04 (s, 3H), 3.16-3.43 (m, 7H), 3.52-3.80 (m, 7H), 4.76 (d, *J* = 10.5 Hz, 1H), 5.05 (dd, *J* = 12.5, 6.7 Hz, 1H), 5.96 (dd, *J* = 15.6, 6.7 Hz, 1H), 6.08 (d, *J* = 12.5 Hz, 1H), 6.21 (d, *J* = 10.2 Hz, 1H), 6.35 (dd, *J* = 15.6, 10.3 Hz, 1H), 7.22-7.37 (m, 5H), 8.35 (s, 1H), 8.76 (s, 1H), 14.51 (s, 1H). ^{13}C NMR (75 MHz, $CDCl_3$): δ 7.7, 8.8, 10.4, 11.1, 20.4, 21.0, 21.6, 30.6, 32.8, 33.0, 33.8, 37.5, 37.7, 38.2, 51.0, 51.1, 57.0, 58.5, 72.7, 73.1, 76.9, 80.0, 90.9, 105.4, 107.3, 108.7, 111.7, 114.9, 115.5, 124.3, 124.7, 127.3, 128.8, 129.0, 130.8, 133.3, 136.1, 140.8, 141.8, 143.6, 156.7, 168.2, 168.3, 171.7, 172.3, 182.3, 193.2.

4.1.2. General protocol used for the parallel synthesis of rifabutin analogs 7-26

Solution A was prepared by solubilizing 3-amino-4-deoxy-4-imino-rifamycin S (400mg, 0.56mmol) in 4mL of THF. Suspension B was prepared by adding Ammonium acetate (128mg, 1.4mmol, 100eq) and zinc (108mg, 1.4mmol, 100eq) in THF (4mL). Solution A and suspension B were stirred vigorously at rt for 30min. Ketones (0.035mmol, 2.5eq) were prepared in separated matrix tubes, then 100µL of suspension B (corresponding to 3.70mg, 0.035mmol, 2.5eq of ammonium acetate and 2.30mg, 0.035mmol, 2.5eq of Zinc) followed by 100µL of solution A (corresponding to 10mg, 0.014mmol of 3-amino-4-deoxy-4-imino-rifamycin S) were added. The reactions were stirred at 40°C. After 30h, the reactions were stopped and controled by LCMS. Solvent was evaporated and the crude material was resolubilized in 500µL of THF. Samples were centrifugated and 100µL of the supernatant were collected and evaporated with Genevac to give the desired analog (corresponding to 2mg, 2.8µmol). The resulting solid was used for testing without further purification. The characterization of analogs 7-26 is described in supplementary data in table S1.

4.2. Biological evaluation

4.2.1. Growth inhibition activity

MICs against *A. baumannii* and *S. aureus* were determined using a microbroth dilution protocol according to the Clinical and Laboratory Standards Institute (CLSI) guidelines. For MIC determinations against *A. baumannii*, RPMI 1640 medium supplemented with 10% FCS was used instead of standard CAMHB. Briefly, a 2-fold dilution series of the compounds was prepared directly in the 96-well assay plate using a digital dispenser. 100 µL of a bacterial suspension prepared at $5x10^5$ CFU/mL in the respective medium was added to the compounds and the plates were incubated without shaking at

35 °C for 20 hours. The MIC was determined visually as the lowest concentration of a compound that prevents visible growth of the bacteria.

The *A. baumannii* strain HUMC1 and *S. aureus* USA300 strain UAMS-1625 were used as reference strains in MIC determinations, while the *A. baumannii* strains with mutations in RpoB or FhuE were previously described.[14]

4.2.2. Transcription inhibition activity

Transcription inhibition activity was determined using cell-free extracts from *A. baumannii* HUMC1.

The cell-free extracts were prepared following a detailed protocol that was previously described.[28] Briefly, a fresh liquid culture of *A. baumannii* HUMC1 was prepared in 2xYT + P medium (16 g/L tryptone, 10 g/L yeast extract, 5 g/L sodium chloride, 7 g/L potassium phosphate dibasic, 3 g/L potassium phosphate monobasic) and the cells were collected at an OD_{600} of 3. The cells were washed and concentrated to 1 g of cell pellet per mL of washing buffer (50 mM Tris base, 14 mM Mg-glutamate, 60 mM K-glutamate, 2 mM DTT, brought to pH 7.7 with acetic acid) with 4 rounds of centrifugation. The cell suspension was subsequently sonicated for 2 min with 10 s on/off intervals and the cell lysate supernatant was collected after centrifugation. The runoff reaction was performed by incubating the lysate for 80 min at 37 °C with shaking and the clear lysate was collected after centrifugation. The obtained clarified extracts were finally dialyzed against dialysis buffer (5 mM Tris base, 14 mM Mg-glutamate, 60 mM K-glutamate, 1 mM DTT, pH 8.2) for 3 h at 4 °C and the dialyzed extracts recovered after a last centrifugation step were stored at -80 °C as 100 µL aliquots until used.

The conditions for determination of cell-free transcription inhibition activity were adapted from a previously detailed protocol.[28] The Nano-Glo Luciferase Assay Substrate (Promega, N1110) and a reporter plasmid (pVT784) expressing the nanoluciferase (NanoLuc) from the constitutive P*trc* promoter were used to monitor the transcription reaction. The reactions were prepared on ice in triplicate on a 10 µL scale in white 384 well plates. The reaction mixture containing the buffer (with all the transcription and translation reagents[28]), the *A. baumannii* extract at 1.2 mg/mL and the compound to be tested was incubated for 30 min before initiation of the reaction with the addition of the reporter plasmid (0.5 nM). The luminescence was measured after 60 min incubation at 25 °C using a Tecan infinite F500 plate reader. The compounds were tested from 8 to 0.002 mg/L and the luminescence values normalized to the no compound control were used to determine transcription IC_{50}s of the compounds using GraphPad Prism.

4.2.3. Accumulation assay

Cultivation of bacteria and treatment with antibiotics. *A. baumannii* HUMC1 (wildtype) and *A. baumannii* HUMC1 Δ*fhuE* were cultured in RPMI 1640 medium supplemented with 10% FCS or in CAMHB. Overnight cultures were used to prepare bacterial suspensions with an OD_{600} of 0.2 in baffled flasks and incubated until an OD_{600} of 0.8 was reached. Then, 5 mL bacterial suspension was transferred immediately to a 15 mL Falcon tube, and 5 µL antibiotic stock solution (0.002 - 5 mM in DMSO) was added. The suspension was incubated at 37 °C for 10 minutes while shaking at 150 rpm. Following this, the bacterial cells were harvested by centrifugation (4500 *g*, 4 °C, 10 minutes).

Generation of whole cell (WC) lysates. The generation of WC lysates was adapted from a procedure previously reported.[24] Briefly, the bacterial pellet was resuspended in 1 mL TBS (50 mM Tris [pH 7.0], 135 mM NaCl, 2.5 mM KCl) and the suspension was transferred to a 2 mL Eppendorf tube. Following

a washing step with 300 µL TBS, the pellet was resuspended in 100 µL TBS. An equal volume of SE-buffer (25 mM Tris, [pH 7.4], 40% (w/w) sucrose, 2 mM EDTA) was added carefully to the bottom of the tube. The resultant phases were mixed by first tapping and then inverting the tube. Following 5 minutes incubation at room temperature, the bacterial cells were pelleted (3500 *g*, 4 °C, 10 minutes) and the supernatant was carefully removed and discarded. 200 µL TS-buffer (25 mM Tris, [pH 7.4], 20% (w/w) sucrose) was added, ensuring not to disturb the pellet. The sample was centrifuged (3500 *g*, 4 °C, 2 minutes), and the supernatant was carefully removed and discarded. Finally, the pellet was resuspended in 190 µL 10 mM Tris [pH 7.4] on ice. All samples were sonified twice using a Bandelin Sonopuls mini20 sonifier equipped with a MS 2.5 tip by applying an 80% pulse corresponding to 1.0 kJ. 10 µL DNase-mix (1 M $MgCl_2$, 60 µg/mL DNase I) was added to the lysate and the lysates were incubated at 37 °C for 15 minutes while shaking at 500 rpm. All samples were stored at -20 °C until further processing for LC-MS/MS analysis.

Subcellular fractionation. The initial sample preparation steps were identical to those described for the generation of WC lysates up until the TS-buffer wash step. 200 µL 0.5 mM $MgSO_4$ (pre-cooled on ice) was carefully layered onto the pellet and the sample was incubated on ice for 10 minutes. After this time, the periplasmic fraction was liberated by centrifugation (3500 *g*, 4 °C, 10 minutes) and collected. The pellet was washed with 200 µL 0.5 mM $MgSO_4$, resuspended in 190 µL 10 mM Tris and the sample sonified as described above. Following the addition of 10 µL DNase-mix and incubation, the cytoplasm was released by high-speed centrifugation (30000 *g*, 45 minutes) and collected. The pellet (containing both the inner and outer membrane) was washed with 200 µL 10 mM Tris and finally resuspended in 200 µL 0.5 mM $MgSO_4$.

Sample preparation and LC-MS/MS analysis. In a 2.2-mL 96 deep-well plate (Brand, BR701354), 80 µL WC sample was combined with 320 µL diluent (1:1.5:1.5 2% formic acid: CH_3CN: CH_3OH). In the case of WC lysates used for the preparation of standards for quantification, the diluent was spiked with preset concentrations of compound. The plate was sealed immediately and its contents mixed using a MixMate set to 900 rpm, 10 °C for 10 minutes prior to centrifugation (2250 *g*, 60 min, 4 °C). Using a Bravo Automated Liquid-Handling Platform (Agilent Technologies, Santa Clara, CA, USA), 320 µL supernatant were transferred to a 96-well plate with V-shaped bottom (Greiner Bio-One, 651201) and dried by vacuum centrifugation using a refrigerated CentriVap with a −80 °C cold trap (Labconco, Kansas, MO, USA). The dry residues were dissolved in 50 µL 3:3:4 CH_3CN: CH_3OH:H_2O containing 0.1% formic acid and 10 ng/mL caffeine as internal standard. Processed samples were analyzed on a 1290 Infinity II Liquid Chromatography System (Agilent Technologies, Santa Clara, CA, USA) coupled to an AB SCIEX QTrap 6500 triple quadrupole mass spectrometer (AB SCIEX Germany GmbH, Darmstadt, Germany). LC separations were achieved using a Gemini 3 µm NX-C18 110 Å 50 mm x 2 mm column (Phenomenex, Torrance, CA, USA) held at 50 °C. A gradient using solvent A (H_2O + 0.1% formic acid) and solvent B (acetonitrile + 0.1% formic acid) at a constant flow rate of 0.8 mL/min was used: 0.00-1.00 minutes 95% A, 5% B; 1.00-5.00 minutes 95% to 5% A, 5% to 95% B; 5.00-6.00 minutes 5% A, 95% B. A multiple reaction monitoring experiment was used for the detection of antibiotics. The Q1/Q3 transition masses were determined in positive mode (see Supplementary Information, Table S3). LC-MS/MS data were processed using the Skyline Software Package:the peak areas of the quantifier peaks normalized to the internal caffeine standard were determined.[29] The standard curves (supplement, Figure S8 to Figure S18) were obtained by measuring the compound-spiked WC matrix and plotting the compound concentration in µM against peak areas normalized to the internal standard. Linear regression analysis was performed with

adequate weighting as indicated (where applicable, see supplement Figure S8 to Figure S18), the concentration of compound in the samples was determined and the data was plotted using GraphPad prism.

5. ACKNOWLEDGMENTS

This research was financially co-funded by European Union under the European Regional Development Fund (ERDF), by the Hauts De France Regional Council (Contract n°NP0020070) and by I-Site ULNE (ANR-16-IDEX-0004 ULNE). The compound management was supported by ChemBioFrance through the ARIADNE platform (Lille, France). Authors also thank the University of Lille, Inserm, Institut Pasteur de Lille and UFR3S for their support. The graphical abstract was created with BioRender.com.

6. SUPPLEMENTARY DATA

Supplementary data to this article can be found online at xx.

7. REFERENCES

1. Paul, M. et al. European Society of Clinical Microbiology and Infectious Diseases (ESCMID) guidelines for the treatment of infections caused by multidrug-resistant Gram-negative bacilli (endorsed by European society of intensive care medicine). Clin. Microbiol. Infect. 28, 521–547 (2022).
2. Tamma, P. D. et al. Infectious Diseases Society of America Guidance on the Treatment of AmpC β-Lactamase–Producing Enterobacterales, Carbapenem-Resistant Acinetobacter baumannii, and Stenotrophomonas maltophilia Infections. Clin. Infect. Dis. 74, 2089–2114 (2022).
3. Lawandi, A., Yek, C. & Kadri, S. S. IDSA guidance and ESCMID guidelines: complementary approaches toward a care standard for MDR Gram-negative infections. Clin. Microbiol. Infect. 28, 465–469 (2022).
4. Murray, C. J. et al. Global burden of bacterial antimicrobial resistance in 2019: a systematic analysis. The Lancet 399, 629–655 (2022).
5. Du, X. et al. Predictors of mortality in patients infected with carbapenem-resistant Acinetobacter baumannii: A systematic review and meta-analysis. Am. J. Infect. Control 47, 1140–1145 (2019).
6. Cassini, A. et al. Attributable deaths and disability-adjusted life-years caused by infections with antibiotic-resistant bacteria in the EU and the European Economic Area in 2015: a population-level modelling analysis. Lancet Infect. Dis. 19, 56–66 (2019).
7. Butler, M. S. et al. Analysis of the Clinical Pipeline of Treatments for Drug-Resistant Bacterial Infections: Despite Progress, More Action Is Needed. Antimicrob. Agents Chemother. 66, e0199121 (2022).
8. Tacconelli, E. et al. Discovery, research, and development of new antibiotics: the WHO priority list of antibiotic-resistant bacteria and tuberculosis. Lancet Infect. Dis. 18, 318–327 (2018).
9. Luna, B. et al. A nutrient-limited screen unmasks rifabutin hyperactivity for extensively drug-resistant Acinetobacter baumannii. Nat. Microbiol. 5, 1134–1143 (2020).
10. Trebosc, V., Kemmer, C., Lociuro, S., Gitzinger, M. & Dale, G. E. Rifabutin for infusion (BV100) for the treatment of severe carbapenem-resistant Acinetobacter baumannii infections. Drug Discov. Today 26, 2099–2104 (2021).
11. Antraygues, K. et al. Design and synthesis of water-soluble prodrugs of rifabutin for intraveneous administration. Eur. J. Med. Chem. 114515 (2022) doi:10.1016/j.ejmech.2022.114515.
12. Campbell, E. A. et al. Structural mechanism for rifampicin inhibition of bacterial rna polymerase. Cell 104, 901–912 (2001).
13. Vaara, M. Comparative activity of rifabutin and rifampicin against gram-negative bacteria that have damaged or defective outer membranes. J. Antimicrob. Chemother. 31, 799–801 (1993).
14. Trebosc, V. et al. In vitro activity of rifabutin against 293 contemporary carbapenem-resistant Acinetobacter baumannii clinical isolates and characterization of rifabutin mode of action and resistance mechanisms. J. Antimicrob. Chemother. 75, 3552–3562 (2020).

15. Dale, G. E. et al. In vivo efficacy of BV100 in mouse models of Acinetobacter baumannii infection. ECCMID 2021 accepted abstract (Poster number 01002). (2021).
16. Lee, B. et al. In Vitro Activity of Rifabutin and Rifampin against Antibiotic-Resistant Acinetobacter baumannii, Escherichia coli, Staphylococcus aureus, Pseudomonas aeruginosa, and Klebsiella pneumoniae. mSphere 6, e00920-21 (2021).
17. Aristoff, P. A., Garcia, G. A., Kirchhoff, P. D. & Showalter, H. D. Rifamycins--obstacles and opportunities. Tuberc. Edinb. Scotl. 90, 94–118 (2010).
18. Artsimovitch, I. et al. Allosteric Modulation of the RNA Polymerase Catalytic Reaction Is an Essential Component of Transcription Control by Rifamycins. Cell 122, 351–363 (2005).
19. Barluenga, J. et al. New rifabutin analogs: Synthesis and biological activity against Mycobacterium tuberculosis. Bioorg. Med. Chem. Lett. 16, 5717–5722 (2006).
20. Albano, M. et al. In Vitro Activity of Rifampin, Rifabutin, Rifapentine, and Rifaximin against Planktonic and Biofilm States of Staphylococci Isolated from Periprosthetic Joint Infection. Antimicrob. Agents Chemother. 63, e00959-19 (2019).
21. Williams, K. J. & Piddock, L. J. Accumulation of rifampicin by Escherichia coli and Staphylococcus aureus. J. Antimicrob. Chemother. 42, 597–603 (1998).
22. Campbell, E. A. et al. Structural, functional, and genetic analysis of sorangicin inhibition of bacterial RNA polymerase. EMBO J. 24, 674–682 (2005).
23. Mosaei, H. et al. Mode of Action of Kanglemycin A, an Ansamycin Natural Product that Is Active against Rifampicin-Resistant Mycobacterium tuberculosis. Mol. Cell 72, 263-274.e5 (2018).
24. Prochnow, H. et al. Subcellular Quantification of Uptake in Gram-Negative Bacteria. Anal. Chem. 91, 1863–1872 (2019).
25. Muñoz, K. A. & Hergenrother, P. J. Facilitating Compound Entry as a Means to Discover Antibiotics for Gram-Negative Bacteria. Acc. Chem. Res. 54, 1322–1333 (2021).
26. Vergalli, J. et al. Porins and small-molecule translocation across the outer membrane of Gram-negative bacteria. Nat. Rev. Microbiol. 18, 164–176 (2020).
27. Zgurskaya, H. I. & Rybenkov, V. V. Permeability barriers of Gram-negative pathogens. Ann. N. Y. Acad. Sci. 1459, 5–18 (2020).
28. Silverman, A. D., Kelley-Loughnane, N., Lucks, J. B. & Jewett, M. C. Deconstructing Cell-Free Extract Preparation for in Vitro Activation of Transcriptional Genetic Circuitry. ACS Synth. Biol. 8, 403–414 (2019).
29 MacLean, B. et al. Skyline: an open source document editor for creating and analyzing targeted proteomics experiments. Bioinformatics, 26, 7, 966–968 (2010).